Systemic Influence in Structural Breaks: Granular Time Series Detection

So Jin Lee *
University of Mannheim

December 1, 2024

to the latest version

Abstract: In a system represented by panel data, a break in the cross-correlation structure can empirically indicate volatility propagation from individual (idiosyncratic) dimensions to the entire system. Individual units contributing the most to this break can act as systemic risk components, potentially driving further instability across the system. We propose a novel method to detect these main contributors — referred to as 'granular units'— as an initial screening tool for potential systemic risk components. Assuming a standard approximate latent factor structure to model system covariance dynamics agnostically, we introduce a straightforward influence measure to evaluate the contributions of individual (idiosyncratic) second moments to the structural break. We also propose a new estimation method for identifying the dates of the structural breaks. Applied to S&P 100 daily return data across major economic crisis periods, the proposed detection scheme effectively identifies likely sources of systemic risk from early crisis stages.

* E-mail: sojin.lee@uni-mannheim.de I would like to express my sincere gratitude to: my supervisor Carsten Trenkler; Christian Brownlees; Otilia Boldea, Juan J.Dolado, Christoph Rothe; Pavel Čížek, Denis Kojevnikov, Bas Werker, Weihao Chen, and TiSEM members; Antonio Cabrales, Juan Carlos Escanciano, Jesús Gonzalo, Nazarii Salish, Carlos Velasco, Andrey Ramos, Alejandro Puerta, and UC3M Dept.of economics members; Matteo Barigozzi; Rebekka Buse and the organizers and participants of HKMetrics 2022; Daniele Bianchi, Maria Grith, Daniele Massacci, Rosnel Sessinou, the organizers and the participants of the FinEML 2023 conference; André Santos, Martina Zaharieva, and seminar participants in Dept.of Quantitative Methods, CUNEF; Mathias Dewatripont, Marc Hallin, George Kirchsteiger, Luca Paolo Merlino, Davy Paindaveine, and the members and the seminar participants in ECARES, Université Libre de Bruxelles; Tsung-Hsien Li, Geert Mesters, and the organizers and the participants of SETA2024 conference; Antonio Ciccone, Matthias Meier, Nicolas Schutz; Giovanni Ballarin, Thibault Cézanne, and Lukas Hack.

1 Introduction

In many economic systems, there is a set of individuals having a system-wide influence. Individual or micro-level idiosyncratic volatilities can translate or propagate to the entire system (Acemoglu, Carvalho, Ozdaglar, and Tahbaz-Salehi (2012), Baqaee (2018), Gaubert and Itskhoki (2021)) by affecting existing relations (Acemoglu and Tahbaz-Salehi (2020), Taschereau-Dumouchel (2019), Heipertz, Ouazad, and Rancière (2019)). The pioneering work of Gabaix (2011) termed an economic system under the systemic influence of such individuals as a *granular economy*. We thus label these individuals *granular units*.

The fundamental characteristic of granular units is described in terms of the impact of individual idiosyncratic second moments on the system second moments. In a system represented by panel data, a change in the cross-correlation structure can empirically indicate the volatility propagation in action from individual (idiosyncratic) dimensions to the entire system. Individual units whose idiosyncratic second moments contribute the most to this change can act as systemic risk components, potentially driving further instability across the system.

We propose a novel detection scheme for detecting these main contributors (the *granular units*), featuring a new estimation method to identify the dates of structural breaks. Applied to S&P 100 daily return data across historical economic crisis periods, the proposed detection scheme effectively identified probable sources of systemic risk from early stages of each crisis. For instance, during the 2007-2008 period, this method highlights notable units that foreshadowed or triggered major financial instability — such as Lehman Brothers, Bear Stearns, and Washington Mutual — as granular units. Those units were identified already in late 2007 and early 2008 before any major collapse occurred.

The first contribution of this project is that it offers a straightforward analysis of the second-moment effects from individual (idiosyncratic) components to the system compared to existing studies. The implementation will also be relatively simple, utilizing established methods of principal component analysis (PCA). The second contribution is that our method operates on a clear and conservative definition of systemic influence. We define an individual-level effect as systemic when it substantially contributes to the system-wide structural break. This definition minimizes debate about whether certain individuals' influences are truly system-wide. Finally, we provide a clear interpretation that connects a standard factor model to a latent network model. From this perspective, our criterion of detection identifies individuals who shape overall equilibrium actions through an underlying latent network.

The proposed granular unit detection scheme can have extended applications. While the

current paper naturally interprets cross-sectional units as individual entities, such as firms or banks, in principle, the units can represent any collection of time-varying variables. For example, if these variables include real and financial variables, the detection scheme can identify which types contribute most to potential system-wide instabilities.

From a methodological perspective, we adopt an agnostic and minimalistic approach to modeling system covariance dynamics by assuming a latent factor structure, with the aim of developing a straightforward screening device for granular units. Although the system is represented by an observable panel, the common factors and their transmission mechanism (i.e., factor loadings) that account for the primary correlation structure may be unknown or unobservable, placing this within the framework of unobservable factor models. We employ a standard approximate factor model, which has been a prominent workhorse in the field of macroeconomics and finance (e.g., Ross (1976), Chamberlain and Rothschild (1983), Stock and Watson (2002a), Stock and Watson (2002b), and Bernanke, Boivin, and Eliasz (2005)) to describe the covariance dynamics at discrete steps.

Among the various types of structural information that the factor model contains, the directional information of the transmission rule – the way latent common factors of unit signal strengths are loaded to the entire units of the system – and its dynamics can truly capture the underlying mechanism of volatility transmission. While the common factor signals or their dynamics can be systematic and detached from micro-level characteristics in nature, the idiosyncratic volatilities of the granular units may propagate by shifting this directional transmission rule. This study focuses on breaks in this distributive characteristic of the system and proposes a straightforward approach to analyze individual units' contributions to such structural breaks. We evaluate a distributive consequence of the idiosyncratic second moments through an interconnected structure. This approach provides a more comprehensive perspective on systemic influence compared to methods that focus solely on the magnitude of the idiosyncratic volatilities or network structures.

From a more technical standpoint, the analysis centers on the factor space – the column space of the factor loading matrix – which encapsulates the directional characteristic. Compared to conventional objects such as aggregate volatility, the factor space represents eigenspace information (of the common component covariance), not the eigenvalues. Utilizing this less traditional object – well-established in the literature for its identification (e.g., Fan, Liao, and Mincheva (2013)) – enables a more direct approach to systemic influence analysis. Our approach shows that the idiosyncratic second moments and the concentration matrix (the partial correlation network) factor the magnitude of the structural break. Then, each unit's systemic influence can be evaluated by the first-order effect of its idiosyncratic second moments on the magnitude of the structural break via a

straightforward application of matrix calculus.

There are two branches of studies related to the aim and the theme of this project. The first branch primarily studies group identification via systemic influence in a stationary environment, e.g., Diebold and Yılmaz (2014), Basu, Shojaie, and Michailidis (2015), Parker and Sul (2016), Barigozzi and Hallin (2017), Barigozzi and Brownlees (2019), Brownlees and Mesters (2021), Guðmundsson and Brownlees (2021), Brownlees, Guðmundsson, and Lugosi (2022). Departing from this literature, this project focuses on a distribution-changing effect from the 'individual' (idiosyncratic) dimension. The second branch of the studies connects group identity to potentially non-stationary system-wide changes as well, e.g., Billio, Getmansky, Lo, and Pelizzon (2012), Bianchi, Billio, Casarin, and Guidolin (2019), Basu and Rao (2021). Modeling and methods for addressing non-stationarity can be complex in this branch of literature.

Our detection scheme can be applied when reliable breakpoint information is available, either from direct acquisition or estimation. In applications, this scheme effectively identifies likely sources of well-known economic crises—such as the dot-com bubble and the 2007-2008 financial crisis—from their early stages, using our breakpoint estimation method. The estimated breakpoints generally align with the common component breakpoints identified by Barigozzi, Cho, and Fryzlewicz (2018). For granular unit identification, results are compared to the partial correlation network-based approach studied in Brownlees and Mesters (2021). We found that the granular units detected by our own method are better interpreted as the potential key sources within the historical context of each crisis.

This paper is organized as follows. In Section 2, we model a dynamic system covariance that incorporates a generic connection to the idiosyncratic second moments. Our measure of systemic influence is introduced in Section 3, where we also propose the detection criteria. Section 4 details the estimation strategy for constructing the proposed influence measure, with or without prior knowledge of structural breakpoints. Section 5 presents an implementation using simulated data for granular unit detection and breakpoint estimation. Applications to daily stock return data, considering both known and unknown structural breakpoints, are discussed in Section 6. Finally, Section 7 concludes with closing remarks.

Notation. The following norms for a matrix M or a vector $\mathbf{v}$ are employed: For a matrix M, denote the Frobenius norm $\|M\|_F \equiv \sqrt{\mathrm{tr}(M'M)}$, and the max norm $\|M\|_{max} \equiv \max_{ii'} |M_{ii'}|$. To streamline notation, we use the expression $\|\cdot\|$ in two ways. For a vector $\mathbf{v}$, it denotes the ℓ_2 norm $\|\mathbf{v}\| = \|\mathbf{v}\|_2 \equiv \sqrt{\mathbf{v}'\mathbf{v}}$. For a matrix M, it denotes the operator

norm $\|M\| = \|M\|_{op} \equiv \sqrt{\lambda_{max}(M'M)}$, the matrix norm induced by the ℓ_2 norm.
A superscript $\perp$ on a vector subspace W denotes the orthogonal complement in terms of the Euclidean inner product in N–dimensional space, $W^\perp \equiv \left\{\mathbf{v} \in \mathbb{R}^N \,|\, \mathbf{v}'\mathbf{w} = 0,\ \forall \mathbf{w} \in W\right\}$. For a column augmentation P of orthonormal basis vectors of W, $P^\perp$ (or $P_\perp$) denotes a column augmentation of basis vectors of the orthogonal complement $W^\perp$ such that $P^\perp P^{\perp\prime} = I - PP'$. The projector will at times be shorthanded by $\mathcal{P} = PP'$ and $\mathcal{P}^\perp = P^\perp P^{\perp\prime}$ for simplicity.
The symbol $\mathcal{N}$ denotes the set of all cross-section indices, $\{1, \ldots, N\}$. The letter i is reserved for the cross-sectional index, while j is for the regime index. Subscripts in the form of $N_r \times N_c$ denote the row (N_r) and column (N_c) dimensions of a matrix. A single subscript implies $N_r = N_c$. For a rank K real matrix $P_{N\times K}$, the linear space spanned by the column vectors $\{\mathbf{p}^k\}$ of P is denoted by $\text{span}(P) \equiv \left\{ \sum_{k=1}^K r_k \mathbf{p}^k \,|\, r_k \in \mathbb{R} \right\}$.

2 Structural Break in a System with Latent Factors

Systemic influence can be understood as a factor behind large breaks in the system cross-correlation structure. Types of idiosyncratic second moments – such as the idiosyncratic volatilities, the cross-sectional or partial correlations – can represent the individual-originated sources that contribute to a structural break in the system's second moments. We aim for a straightforward analysis of a second-moment to second-moment effect from individuals to the system without specifying the factors of the system covariance. Such analysis is enabled by employing the latent factor model as an intrinsic tool for modeling the structure of system cross-correlations, as we suggest in this section. Additionally, we will discuss how a structural break, captured by changes in the factor space, has a natural interpretation within the context of a generic latent network model.

2.1 Covariance Dynamics and Factor Space Changes

Consider a system of N time series, $\mathbf{y}_t = [y_{1t}, \ldots, y_{Nt}]'$, of a single economic variable, y, of interest, e.g., sales or stock returns. Assume that there is a single set of H important cross-sectional units, referred to as the *granular units*. We aim to identify this set of granular units, $\mathcal{G}$. For simplicity, we can write $\mathbf{y}_t = [\mathbf{y}_{1:H,t}, \mathbf{y}_{H+1:N,t}]'$, where $\mathbf{y}_{1:H,t}$ refers to the values of y_t for the granular units (re-indexed as $\mathcal{G} = \{1, \ldots, H\} \subset \mathcal{N}$), and $\mathbf{y}_{H+1:N,t}$ refers to the values of the remaining, i.e., the non-granular units.
The system covariance evolves in discrete steps. There are two regimes before and after one break, respectively: the present (regime 0) and the future (regime 1). Let $\mathtt{I}_0$ denote

the time window of the present regime, and $\mathtt{I}_1$ the time window of the future regime. We can now formalize our benchmark model.

2.1.1 Benchmark Model and Assumptions

For each $j \in \{0, 1\}$, let $\mathbf{y}_t$ be decomposed into common component $\boldsymbol{\chi}_{j,t}$ and idiosyncratic component $\mathbf{u}_t$, such that:

$$\mathbf{y}_t = \boldsymbol{\chi}_{j,t} + \mathbf{u}_t, \quad \text{where} \quad \mathbf{u}_t = [\mathbf{g}_t \quad \boldsymbol{\epsilon}_t]' \quad \text{for all } t \in \mathtt{I}_j. \tag{1}$$

Here, $\mathbf{g}_t$ denotes idiosyncratic components of the granular units, and $\boldsymbol{\epsilon}_t$ denotes idiosyncratic components of the non-granular units. Further, $\mathbf{y}_t$, $\boldsymbol{\chi}_{j,t}$ and $\mathbf{u}_t$ are all mean-zero objects, specific to regime j. We impose the following assumptions:

Assumption 1. $\Sigma_{y,j} = \Sigma_{\chi,j} + \Sigma_{u,j}$, where $\Sigma_{\chi,j} = P_j \Lambda_{\chi,j} P_j'$ with $K_j \ll N$ non-zero eigenvalues $\lambda_{\chi,j,k} = O(N)$ for $\Lambda_{\chi,j} = \text{diag}(\lambda_{\chi,j,k})_{k=1,\dots,K_j}$, and $P_j' P_j = I_{K_j}$.

Assumption 2. There exists a constant $q_j \in [0, 1]$ such that

$$c_{u,j} \equiv \max_{i=1,\dots,N} \sum_{i'=1,\dots,N} |\text{cov}(u_{it}, u_{i't})|^{q_j} = O(1).$$

Assumption 3. $\|P_0 P_0' \Sigma_{u,0} P_0^{\perp} P_0^{\perp\prime}\|_F = o(1)$.

Assumption 4. $\Sigma_{y,1} = \Sigma_{y,0} + Z$, where $\|P_0' Z P_0^{\perp}\|_F = O(N)$.

The expression (1), supported by Assumptions 1 and 2, states that, in each regime, $\mathbf{y}_t$ is decomposed into two components: the common component with low dimensional large and dominant variances and the idiosyncratic component with bounded variances. A system has a factor structure if it has this decomposability.

Assumptions 1 and 2 are standard conditions for the approximate factor model that guarantee the decomposability. The idiosyncratic components can be correlated but in a bounded fashion for any size of the cross-sectional dimension N, as stated in Assumption 2. On the other hand, the common components prevail no matter how large the system is, following Assumption 1. $\Sigma_{\chi,j} = P_j \Lambda_{\chi,j} P_j'$ is the spectral decomposition of the common component covariance.[1] As captured by the unbounded non-zero eigenvalues of $\Sigma_{\chi,j}$, the

[1] Equivalently, it is the (thin) singular value decomposition of $\Sigma_{\chi,j}$.

size of common component covariance is not dissipating in large N limit.[2]

The major correlation structure of the system is captured by a small number, K_j, of important directions $\{\mathbf{p}_j^k\}_{k=1,\dots,K_j}$, which load the non-dissipating eigenvalues. If we assume there are K_j independent signals of strength $\{\lambda_{\chi,j,k}\}_{k=1,\dots,K_j}$, these directions represent how those signals are distributed to the entire $N-$dimensional cross-sectional units. When the signals are unobservable, this directional information[3] is encapsulated by the factor space, as defined below.

Factor Space. The factor space of regime j is the eigenspace of the common component covariance $\Sigma_{\chi,j}$ in $N-$ dimension, that is,

$$\text{span}(P_j) \equiv \text{Col}(P_j) = \Big\{ \sum_{k=1}^{K_j} r_k \mathbf{p}_j^k \,|\, r_k \in \mathbb{R} \Big\}. \tag{2}$$

In the next subsection, we review how focusing on the factor space provides a straightforward way to analyze factor loading dynamics, aligned with the standard specification of the common component – $\boldsymbol{\chi}_{j,t} = B_j \mathbf{f}_{t,j}$, where $f_{t,j}$ denotes common latent factor signals and B_j represents a static rule of loading the common signals onto the system.[4] Here, we first continue our discussion of the benchmark assumptions, for which a description of the conventional loading-signal specification is not strictly necessary.

Under Assumptions 1 and 2 with a perturbation bound result (the $\sin\theta$ theorem) of Davis and Kahan (1970), the eigenspace of the K_j- leading eigenvalues of the system covariance $\Sigma_{y,j}$ is consistent with the factor space at the population level.

Assumption 3 guarantees that $\Sigma_{y,j}$ is asymptotically block diagonal with respect to the factor space basis. Assumption 4 hypothesizes that the regime-0 covariance experiences a substantial perturbation that is off-diagonal with respect to the previous basis $[P_0\ P_0^{\perp}]$. Let $P_j^{\perp}$ denote the column augmentation of $N-K_j$ basis vectors of the space $\text{span}(P_j)^{\perp} = \big\{v \in \mathbb{R}^N \,|\, v'p = 0,\ \forall p \in \text{span}(P_j)\big\}$, the orthogonal complement of the factor space $\text{span}(P_j)$. Then, up to an error E of order $o(1)$ (note that $\|E\|_{\max} = \max_{i,i'} |E_{ii'}| = o(1)$ by Assumption

[2]Although there is a natural explanation – Wang and Fan (2017) equation (1.1) – the rate is assumed to be linear in N mainly to simplify the later discussion. This can be easily generalized.

[3]Such directional information can be interpreted in terms of network centrality. We will discuss this further in a later part of the section.

[4]The static representation can also allow for a latent dynamic factor signal process with a finite lag under standard regularity conditions, see Forni, Giannone, Lippi, and Reichlin (2009).

3) for large N, the regime-0 covariance can be written in terms of P_0 as

$$\Sigma_{y,0} \simeq \begin{bmatrix} P_0 & P_0{}^{\perp} \end{bmatrix} \begin{bmatrix} \Lambda_{1,0} & \mathbf{0}_{K_0,N-K_0} \\ \mathbf{0}_{N-K_0,K_0} & \Lambda_{2,0} \end{bmatrix} \begin{bmatrix} P_0{}' \\ P_0^{\perp\prime} \end{bmatrix}. \tag{3}$$

Due to the assumed perturbation, a sizable perturbation $P_0{}'ZP_0{}^{\perp}$ (and $P_0{}^{\perp\prime}ZP_0$) will be added to the initially zero off-diagonal blocks in the expression (3). After such a perturbation, the previous important directions (or a basis of the regime-0 factor space) P_0 can no longer explain the system's major correlation structure. The new regime will thus admit a new set of important directions represented by P_1 such that

$$\Sigma_{y,1} \simeq \begin{bmatrix} P_1 & P_1{}^{\perp} \end{bmatrix} \begin{bmatrix} \Lambda_{1,1} & \mathbf{0}_{K_1,N-K_1} \\ \mathbf{0}_{N-K_1,K_1} & \Lambda_{2,1} \end{bmatrix} \begin{bmatrix} P_1{}' \\ P_1^{\perp\prime} \end{bmatrix}, \tag{4}$$

which implies that the factor space has changed from span(P_0) to span(P_1). Appendix B contains further discussion on covariance dynamics and factor space changes, where we explain that the existence of the factor structure in both regimes (Assumptions 1 and 2) also suggests the type of perturbation characterized in Assumption 4.

2.1.2 Identifiable Changes in the Unobservable Factor Loadings

Focusing on the factor space (2) provides a straightforward way to disentangle a structural change of the latent transmission rule (the factor loading) from that of the latent signals (the factors) it carries to the entire $N-$dimensional system. In the conventional specification,

$$\boldsymbol{\chi}_{j,t} = B_j \mathbf{f}_{j,t}, \tag{5}$$

the unobservable factor loading B_j and the signals $\mathbf{f}_{j,t}$ can be identified up to invertible linear transformations. In many studies, substantial breaks in the factor loading matrix have been naturally interpreted as structural changes in the system, reflecting changes in how common macroeconomic (systematic) factors transmit to the entire system.[5] However, as both the factor signals and their loadings are unobservable, dynamics of the factor (signal) covariance $\mathrm{E}[\mathbf{f}_{j,t}\mathbf{f}_{j,t}{}']$ cannot be distinguished from that of the transmission rule without extra restrictions.

[5]For instance, breakpoints correspond to important economic events such as the 1979-1980 oil price shock or the Great Moderation, e.g., in Stock and Watson (2009), Chen, Dolado, and Gonzalo (2014), Ma and Su (2018), and Baltagi, Kao, and Wang (2021). Banerjee, Marcellino, and Masten (2008) and Yamamoto (2016) have provided evidence that consideration of such breaks is important in forecasting.

In our view, it is the directional information of the transmission rule – the way latent common factors of unit signal strengths are loaded to the entire units of the system – and its dynamics that can truly capture the underlying mechanism of volatility transmission. While the common factor signals or their dynamics can be systematic and detached from micro-level characteristics in nature, the idiosyncratic volatilities of the granular units may propagate by shifting this distributive characteristic of the transmission rule. Notably, the dynamics of this directional information of the factor loading can be disentangled from the latent dynamics of the factor signals.

To clarify this, let us recall the representation. The natural way to capture this directional information is to take a column-orthonormal representation of the factor loading matrix, which corresponds to P_j in Assumption 1, up to orthonormal transformations to guarantee invariance under the unobservability. In other words, due to the latent nature of the factor signals, the directional information is represented by a (K_j-dimensional) subspace of the entire $N-$dimension, the factor space (2). It guarantees the necessary invariance, for the representation of which we take the projector $\mathcal{P}_j \equiv P_j P_j{}'$. Indeed, any linear space can be identified by the projector operator that projects any vector onto that space.

A change of the factor space is defined independently from changes in the factor covariance structure. Note that a structural change in the factor covariance, while keeping the number of factors constant, will occur in one of the following two types or as a combination of both. The first type involves a change resulting from a different linear combination of the factors. This is captured by the eigenvector changes of the factor covariance matrix, which corresponds to an internal rotation within the K_j-dimensional subspace. The factor model should remain invariant under this type of change as long as the signals are assumed to be latent. The second type is a change in the factor signal strengths captured by a change in eigenvalues of the factor covariance. Both of the characteristics can be seen as structural changes in the factor signals rather than a change in the transmission rule.

Neither the factor space nor its representation, $\mathcal{P}_j = P_j P_j{}'$ is affected by these types of changes. Projectors remain invariant under the internal rotations – rotations within the K_j dimensional subspace – and the normalization separates out the factor signal strengths. However, the factor space will be affected by a change in the number of factors, which is conceptually expected. The introduction or removal of a factor necessitates the emergence or disappearance of specific pathways of transmission. Hence, the dynamics of the identifiable directional information of the factor loading matrix, as carried by the factor space, can be disentangled from those of the factor signal covariance without

requiring additional restrictions.

2.2 Interpreting Structural Breaks: Factor space, Network centrality, and Equilibrium

To provide a more tangible and interesting interpretation of the structural break that is captured by the factor space change, let us make a slight digression to zoom in on a connection between the standard factor model and a generic network model.[6] Consider a simple network model where $\{y_{it}\}$ are cross-sectionally interconnected by Ω, net of idiosyncratic components during $t \in \mathtt{I}_0$, such that

$$y_{it} - u_{it} = r_t + \sum_{i'} \Omega_{ii'}(y_{i't} - u_{i't}), \quad \text{or equivalently,}$$

$$\mathbf{y}_t = (I_N - \Omega)^{-1}\mathbf{1}r_t + \mathbf{u}_t = \mathbf{b}r_t + \mathbf{u}_t, \tag{6}$$

where we assume the invertibility of $(I_N - \Omega)$. The marginal benefits of exposure to r are assumed to be $\boldsymbol{\alpha}_{N\times 1} = \mathbf{1}$. The general model with multiple common exposures $\{r_k\}_{k=1,\ldots,K}$ with corresponding heterogeneous marginal returns $\{\boldsymbol{\alpha}^k \neq \mathbf{1}\}_{k=1,\ldots,K}$ will be discussed soon.

This class of models can cover broad scenarios of interconnected economic activities. For instance, $\mathbf{y}_t$ can be investment returns balanced with a common return r – from a safe asset investment or a final good demand depending on the context – where Ω can represent mutual investments through a production network or borrower-lender relationships.

On the one hand, in the simple case (6) of a single common exposure r with homogeneous marginal returns,

$$\mathbf{b} = (I_N - \Omega)^{-1}\mathbf{1}, \tag{7}$$

which equals the Bonacich centrality of the cross-sectional units in the constant network Ω (Ballester, Calvó-Armengol, and Zenou (2006)). When the common source of exposure and the network structure Ω are not observable, one can describe (6) by a one-dimensional factor model,

$$\mathbf{y}_t = \tilde{B}f_t + \mathbf{u}_t,$$

where the factor loading $\tilde{B}_{N\times 1}$ amounts to the centrality vector $\mathbf{b}$, and the common factor f_t corresponds to the common source of exposure r_t, up to a unknown scaling. From this point of view, a change of the factor space will be incurred by a structurally substantial change of the centrality, which is more than just a change in the scaling.

[6] Appendix C provides an extended discussion.

On the other hand, Bonacich centrality is a concept closely related to the equilibrium exposure to r given the network structure and the marginal returns (Ballester et al. (2006), Galeotti, Golub, and Goyal (2020)). With marginal benefits $\boldsymbol{\alpha} = [\alpha_i]_{i=1,\dots,N}$ potentially heterogeneous across i for the single exposure r, the weighted Bonacich centrality $\mathbf{b} = [\beta_i]_{i=1,\dots,N} = (I_N - \Omega)^{-1}\boldsymbol{\alpha}$ depicts the equilibrium actions solving

$$\max U_i(b_i) = \max \left[b_i\alpha_i - (1/2)b_i^2 + b_i \sum_{i'} \Omega_{ii'} b_{i'} \right]. \tag{8}$$

In line with this conceptual Bonacich-Nash linkage, the factor space change can be interpreted as a change in equilibrium actions, and the granular units as the main contributors to the change in the equilibrium. We discuss this perspective in more detail in Appendix C for general cases with multiple sources of common exposure $\{r_k\}$ and corresponding marginal benefits $\boldsymbol{\alpha}^k$. In a nutshell, the generic model can be written as

$$\mathbf{y}_t = \left[(I_N - \Omega)^{-1}\boldsymbol{\alpha}^1 | \cdots | (I_N - \Omega)^{-1}\boldsymbol{\alpha}^K \right] \mathbf{r}_t + \mathbf{u}_t = B\mathbf{r}_t + \mathbf{u}_t, \tag{9}$$

where each column of B consists of a weighted Bonacich centrality $\mathbf{b}^k \equiv (I_N - \Omega)^{-1}\boldsymbol{\alpha}^k$ capturing the equilibrium actions of exposure to r_k. When Ω,$\{\boldsymbol{\alpha}^k\}$ and $\{r_k\}$ are latent and $K_0 (\leq K)$ signals of $\{r_k\}$ are strong, (9) will be described by the K_0 dimensional factor model $\mathbf{y}_t = \tilde{B}_{N\times K_0}\mathbf{f}_t + \mathbf{u}_t$, and the factor space carries information of the latent centrality or the equilibrium actions.

3 Systemic Influence in Structural Breaks

For the granular units, idiosyncratic disturbances they experience – whether through their own volatilities or correlations with other units – can trigger a viable adjustment of existing relationships, leading to a change in the major cross-correlation structure. Such adjustments may take time and occur infrequently rather than gradually due to the necessary process of learning, assessment, and implementation. As a result, these adjustments manifest as structural breaks in our framework, identified as discrete changes in the factor space, while remaining agnostic about the exact mechanisms driving them. The systemic importance of the idiosyncratic disturbances of granular units becomes more apparent through these breaks. Within a regime, such disturbances may initially appear sparse and weakly correlated, offering little indication of their potential importance.

The second-moment-to-second-moment effect, from the idiosyncratic dimension to the system, can identify the granular units. We propose a straightforward approach to analyze this effect. First, we show that the idiosyncratic second moments and the concentration

matrix (the partial correlation network) factor the magnitude of the structural break. Subsequently, the systemic influence of each unit can be evaluated by the first-order effect of its idiosyncratic second moments on the magnitude of the structural break via a straightforward application of matrix calculus. In addition, we discuss systemic importance analysis based on the partial correlation network or concentration matrix, comparing it to our approach. Finally, the criteria for detecting the granular unit will be proposed.

3.1 Bridging the Idiosyncratic Dimension and the Structural Break

The magnitude of the structural break – captured by the change of the factor space – can be measured using the following metric:

Projection metric (Edelman, Arias, and Smith (1998))

$$d\big(\text{span}(P_0), \text{span}(P_1)\big) \equiv \text{tr}\big[(I_N - \mathcal{P}_0)\mathcal{P}_1(I_N - \mathcal{P}_0)\big]. \tag{10}$$

It is a distance between two spaces $\text{span}(P_0)$ and $\text{span}(P_1)$. To be precise, in (10), we take the square of the original projection metric as the distance measure. Recall that the spaces are represented by a form of projectors $\mathcal{P}_j = P_j P_j'$, free from any identification issues, as the expressions $P_j P_j'$ are invariant under any choice of the representation of the column orthonormal basis P_j. From now on, we use the terms factor space ($\text{span}(P_j)$) and its projector representation $\mathcal{P}_j$ interchangeably.

The idiosyncratic dimension bridges into a change in the common ("systematic") dimension through the measure (10). Under the benchmark model in Section 2.1.1, the following proposition shows that for a given system with a large cross-sectional dimension N, the size of the break measured by (10) can be expressed as a composition involving the idiosyncratic covariance. Once translated in this way, the contribution of the idiosyncratic second moments to the change in the system's second moments, resulting in the structural break, can be straightforwardly analyzed by applying matrix calculus.

Proposition 1. Under the benchmark model, for large N,

$$d\big(\text{span}(P_0), \text{span}(P_1)\big) = \text{tr}\Big(\Sigma_{u,0}\Sigma_{y,0}^{-1}\mathcal{P}_1\Sigma_{y,0}^{-1}\Sigma_{u,0}\Big) + o(1). \tag{11}$$

The proof is in Appendix A. An intuitive argument is as follows. In a large N limit, the approximate factor model is compatible with PCA representation. For the decomposition

$\Sigma_{y,0} = \Sigma_{\chi,0}+\Sigma_{u,0}$, the factor space $\mathcal{P}_0$ is close to the first (in descending order of eigenvalues) K_0- principal eigenspace of $\Sigma_{y,0}$. The orthogonal directions of $\mathcal{P}_0$ mainly capture the idiosyncratic covariance,

$$(I_N - \mathcal{P}_0)\Sigma_{y,0} \simeq \Sigma_{u,0}.$$

Then,

$$\begin{aligned}(I_N - \mathcal{P}_0)\mathcal{P}_1(I_N - \mathcal{P}_0) &= (I_N - \mathcal{P}_0)\Sigma_{y,0}\Sigma_{y,0}^{-1}\mathcal{P}_1\Sigma_{y,0}^{-1}\Sigma_{y,0}(I_N - \mathcal{P}_0) \\ &\simeq \Sigma_{u,0}\Sigma_{y,0}^{-1}\mathcal{P}_1\Sigma_{y,0}^{-1}\Sigma_{u,0}.\end{aligned}$$

The expression (11) will be utilized to construct a measure of the systemic influence of cross-sectional units in the next section. To simplify the exposition, in the rest of this section, *let us omit the present regime subscripts* 0 (except for the case of the regime-0 factor space or its basis) unless otherwise stated. That is, expressions such as Σ_y^{-1}, Σ_u, or any subcollections of their entries without subscripts will indicate regime-0 objects.

3.2 A Measure of Systemic Influence

An individual unit's systemic influence can be measured by the contribution of its idiosyncratic second moments to the factor space change. The most straightforward way to capture this contribution is through the first-order effect of Σ_u on the magnitude of the factor space change. As the idiosyncratic covariance factors the size of the structural break as in (11), it is simply the partial derivative of the expression (11) with respect to Σ_u,

$$\partial_{\Sigma_u} d\big(\text{span}(P_0), \text{span}(P_1)\big) = 2\Sigma_y^{-1}\mathcal{P}_1\Sigma_y^{-1}\Sigma_u, \tag{12}$$

that captures the contribution. This simple application is enabled by the characteristic of the trace operator, a linear combination of the elements of the matrix components.

The adjusted factor space $\mathcal{P}_1$ is assumed to have no direct (first-order) effect from a hypothetical perturbation on Σ_u. The idiosyncratic disturbances may demand the adjustment of the existing relationships between some or all cross-sectional units. For example, the network structure Ω, within the conceptual connection from the latent network model in Section 2.2. However, the result of the adjustment – the new relationships Ω_1 or the corresponding new factor space $\mathcal{P}_1$ – may have a functional dependence on the parameters that enable the adjustment, for example, the market or bargaining power, information superiority of certain units or system-wide asymmetries of those, rather than on the disturbances that may demand an adjustment. A technical discussion for more general cases continues in Appendix D.

To make a straightforward interpretation of (12), let us assume that all idiosyncratic components are uncorrelated. As Σ_u is diagonal, it is only $\sigma^2_{u,i}$ that matters among the idiosyncratic second moments for given unit i. In this case, the share of unit i in the factor space adjustment is captured by

$$\mathcal{I}_i \equiv \frac{1}{2}\partial_{\sigma^2_{u,i}} d\big(\text{span}(P_0), \text{span}(P_1)\big) = \Big[\Sigma_y^{-1}\mathcal{P}_1\Sigma_y^{-1}\Sigma_u\Big]_{ii} = [\sigma_y{}^{i1} \cdots \sigma_y{}^{iN}]\mathcal{P}_1 \begin{bmatrix} \sigma_y{}^{1i} \\ \vdots \\ \sigma_y{}^{Ni} \end{bmatrix} \sigma^2_{u,i}.$$

The contribution of unit i consists of three types of information. First, the size of the idiosyncratic shock faced by unit i ($\sigma^2_{u,i}$) in regime-0. Second, the importance of unit i in terms of the structure of the partial correlation $[\Sigma_y^{-1}]_i = [(\sigma_y{}^{in})_{n=1,\dots,N}]$ in regime-0.[7] Finally, how all other units connected to i through the partial correlation become important to explain the major cross-correlation structure of the next regime ($\mathcal{P}_1$). Together, these three features convey a full picture of the systemic influence of individuals.

In other words, $\mathcal{I}_i$ evaluates the distributive consequence ($\mathcal{P}_1$) of the idiosyncratic second moments ($\boldsymbol{\sigma}_u^i = [\sigma_u^{i1}, \dots, \sigma_u^{iN}]'$, for general cases) through an interconnected structure (Σ_y^{-1}). This approach provides a more comprehensive perspective on systemic influence compared to methods that focus solely on the magnitude of the idiosyncratic volatilities or a network structure.

For a general structure of the idiosyncratic covariance, we define the contribution of unit i as a norm of the ith column of (12), that is:

$$\mathcal{I}_i \equiv \left\| \frac{1}{2}\big[\partial_{\Sigma_u} d\big(\text{span}(P_0), \text{span}(P_1)\big)\big]^i \right\| = \left\| \Sigma_y^{-1}\mathcal{P}_1\Sigma_y^{-1}\boldsymbol{\sigma}_u^i \right\|, \tag{13}$$

where $\boldsymbol{\sigma}_u^i = [\sigma_u^{i1}, \dots, \sigma_u^{iN}]'$ acts as the source triggering the structural break.

3.2.1 The Concentration Matrix Revisited

In a stationary environment, the concentration matrix alone can be utilized for the detection of granular units. Brownlees and Mesters (2021) showed that a column norm of the concentration matrix Σ_y^{-1} can provide a measure of systemic influence in a stationary environment under a certain type of static factor model.[8] The concentration matrix

[7] In a stationary environment, the concentration matrix alone can be utilized for the detection of granular units. We will soon discuss this point before the end of this subsection.

[8] This expression does not have subscript because the discussion is independent of the existence of different regimes.

is a popular object of study in the literature, as it captures partial correlations among cross-sectional items of stationary panel data.[9] The granular units identified through the concentration matrix can be seen as the most central individuals in the stationary network of partial correlations. In contrast, our proposed modeling assumes a non-stationary environment, where the underlying latent structure governing the cross-correlations is infrequently adjusting. This is as if the adjustment was carried out after assessing a situation by learning during a stationary time window.

Such a "slow" adjustment scenario is more adapted to a high-frequency data environment. In a low-frequency environment, one can assume that the data exhibits a certain static factor structure that already represents the systemic influence. The observations can be made by giving enough time to the system to absorb or get affected by the potential systemic influence. It may not be the case in a high-frequency environment. It can be the case that the effect of the influence is not realized in each high-frequency observation but is exhibited as a systematic change after some period. From our point of view, this latter behavior provides a chance to distinguish a factor behind the perceived structure of correlations. Accordingly, the proposed measure of influence not only involves the partial correlation structure of the current regime but also considers the changed correlation structure of the next regime, realized through P_1 or $\mathcal{P}_1$.

The concentration matrix itself is a form of a partial change of the system covariance as well. By the very nature of the symmetric operator inversion, the (i, i')−th component of Σ_y^{-1} equals (Horn and Johnson (2013), equation (0.8.2.7))

$$[\Sigma_y^{-1}]^{ii'} = \frac{1}{\det \Sigma_y} \frac{\partial}{\partial \sigma_y^{ii'}} \det \Sigma_y = \frac{\partial}{\partial \sigma_y^{ii'}} \ln \det \Sigma_y. \tag{14}$$

It is the percentage partial change of the size of the dispersion of the system covariance measured by $\det \Sigma_y = \prod_{i=1}^N \lambda_i$[10], due to a perturbation on σ_y^{ij}, fixing all other entries of the covariance. The i−th column norm of the concentration matrix corresponds to the sum of the partial effects (14) due to i for overall i', for example,

$$\|\Sigma_y^{-1}\|^i = \sqrt{\sum_{i'=1}^N \left(\frac{\partial}{\partial \sigma_y^{ii'}} \ln \det \Sigma_y \right)^2}.$$

In this sense, it does capture a kind of importance of the individual's second moment to the system's second moments. Assuming a factor structure, however, there are several aspects

[9] A standard exposition can be found in Pourahmadi (2013), Chapter 5.

[10] $\det \Sigma_y$ captures the volume of the image of the system covariance as an operator.

it does not capture. First, if there are idiosyncratic shocks that potentially communicate with the transmission rule of the common factors, their effects can not be fully captured by the partial derivatives. All other $\{\sigma_y^{jk}\}$ will change according to the evolving transmission rule. By keeping them constant, the partial change (14) will miss such an indirect channel that may provide a fuller picture of systemic influence in the non-stationary environment on which we focus. Second, due to the nature of the determinant (defined by eigenvalue information), a measure based on (14) does not actively exploit directional characteristics of the system covariance captured in eigenspaces, which may be informative under a factor structure.

It is worth noting that the focus of current literature has been on the concentration matrix of the residual covariance (Σ_u^{-1}) as well, to capture a conditional partial correlation structure of a system (e.g., Dahlhaus (2000), Eichler (2012), Bianchi et al. (2019), and Barigozzi and Brownlees (2019)). It can represent a contemporaneous dependence conditional on the common factor dimension. When the *conditions* are changing, for example, due to a regime change represented by a change in the factor loading, a disparity between the conditional contemporaneous dependence in different regimes can be important and informative, as mentioned, e.g., in Bianchi et al. (2019) and Massacci (2021). The way we perceive it is that such a change of *condition* will be informative for recognizing a group of systemic individuals.

We will now establish criteria for granular unit detection utilizing the proposed influence measure.

3.3 Criteria for Detecting Granular Units

We have discussed how systemic influence can be evaluated through the contributions of the idiosyncratic second moments to changes of the factor space. Granular units are naturally characterized as individuals who present the largest contributions. This provides the criterion for membership in $\mathcal{G}$, the set of granular units. What remains is to establish a criterion for the size of $\mathcal{G}$. To complete the detection criteria, we will utilize a comprehensive feature of the factor space dynamics.

Recall that granular units are those capable of altering existing relationships in ways that induce major changes in system correlations. The adjustment can be seen as changes of equilibrium exposures to common sources or in network centrality, given a network representing the existing relationships or the within-regime cross-sectional correlations, as discussed in Section 2.2.

When a granular unit adjusts, it induces a reconfiguration of the entire equilibrium actions of all units. For multiple common sources of exposure, $\{r_k\}$, the equilibrium actions ($\mathbf{b}^k_{N\times 1}$) can be defined for each r_k. If the equilibrium actions change for H distinct common sources, we assume there are H granular units. Distinct granular units can be found responsible for changes in equilibrium exposure to each distinct common source. In its latent counterpart – involving the unobservable network, common sources, and potentially unit-specific marginal returns on these sources – this assumption will be framed as a feature of the factor space change, as follows.

Assumption 5. The number of systemic individuals corresponds to the number of independent directions of a change of the factor space. That is,

$$H = \text{rank}(\mathcal{P}_0^{\perp}\mathcal{P}_1). \tag{15}$$

A geometric feature of the factor space dynamics illuminates this assumption. Under the benchmark model introduced in Section 2.1.1, the dynamics are conceptualized as a form of rotation of the regime-0 factor space to the regime-1 factor space.[11] If the factor spaces have a fixed dimension 1, the dynamics will be represented solely by a vector P_0, which, when rotated in a certain direction (say V, the *velocity*) yields another vector P_1 in $N-$dimensional space. Similarly, the motion of a multi-dimensional subspace is described by a collection of rotations of its $K-$basis vectors, each rotating in a specific direction. The velocity also becomes a multidimensional object, represented as a collection of the directions for change.

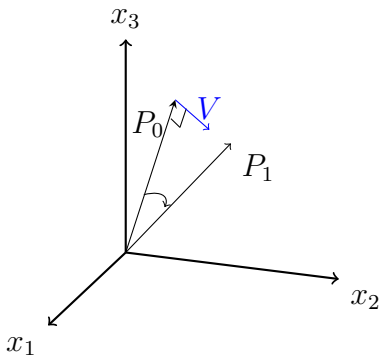

Figure 1: A rotating 1−dimensional factor space in $N = 3$ dimension. P_0 (P_1) represents a basis of the regime 0 factor space span(P_0) (span(P_1), resp.).
(All vectors representing directional information (P_0,P_1, and V) have their lengths normalized to 1.)

Let us recall that, as in the argument inside the trace of (10), the change of the factor space is measured by the component of $\mathcal{P}_1$ that is perpendicular to span(P_0), or $\mathcal{P}_0$. The directional information of this component equals exactly the velocity. The number of

[11] Refer to Appendix B for a detailed discussion.

independent directions of change, or the rank of V, is a crucial characteristic determining the factor space dynamics, just as important as the overall magnitude of the change (10), which is employed to construct the criterion for membership detection. We assume that the number of granular units is equal to the number of directions constituting the velocity V. The factor space evolves as if each systemic individual selects an independent direction of change.

The choice of this velocity is the true latent source of factor space dynamics, which remains almost entirely model-free in our approach. Although the true process behind the directional choice is agnostic, the rank of V, or the rank of the change, can be deduced as long as we have any factor space representations, P_0 and P_1.

3.3.1 Detection Criteria

We can now summarize the criteria for detecting the size (how many systemic individuals there are) and the membership (who the systemic individuals are) of the set of granular units. The statement of the criteria has been assigned a new subsection number for ease of future reference.

Number of Granular Units $H = \mathrm{rank}(\mathcal{P}_0^{\perp}\mathcal{P}_1)$.

Membership of the set of Granular Units The set $\mathcal{G}$ of granular units consists of H cross-sectional units which present the highest column norms,

$$\mathcal{I}_i \equiv \left\| \frac{1}{2}\left[\partial_{\Sigma_u} d\big(\mathrm{span}(P_0), \mathrm{span}(P_1)\big)\right]^i \right\| = \left\| \Sigma_y^{-1}\mathcal{P}_1\Sigma_y^{-1}\boldsymbol{\sigma}_u^i \right\|, \tag{13}$$

where Σ_y^{-1} is the regime-0 concentration matrix and $\boldsymbol{\sigma}_u{}^i = [\sigma_u^{i1}, \ldots, \sigma_u^{iN}]'$ is the i–th column of the regime-0 idiosyncratic covariance.

The sample analogue of (13) will be utilized in practice. In Appendix E, we provide a more detailed explanation of the geometric aspects of the detection criteria.

4 Estimation

The proposed detection scheme exploits a structural break, characterized as a change of the factor space. Although detecting the breakpoint is necessary in principle, the main focus of our discussion, presented in the first section, is on the case where the breakpoints are known. We also address the estimation of breakpoints in the second section. The

systematic analysis of cases involving unknown breakpoints will be explored in detail in a separate project.

4.1 Estimation with a Known Breakpoint

Assume that we know one break point that separates two windows of the present and future regimes, $\mathtt{I}_0$ and $\mathtt{I}_1$. The length of each regime, $|I_j| = \kappa_j T$, for some constant $\kappa_j \in (0,1)$, for the entire time period T. The sample analogue of the proposed influence measure,

$$\hat{\mathcal{I}}_i = \left\| \hat{\Sigma}_{y,0}^{-1} \hat{P}_1 \hat{P}_1{}' \hat{\Sigma}_{y,0}^{-1} \hat{\boldsymbol{\sigma}}_{u,0}^{i} \right\|, \tag{16}$$

consists of the $i-$ th column $\hat{\boldsymbol{\sigma}}_{u,0}^{i}$ of idiosyncratic covariance matrix $\hat{\Sigma}_{u,0}$, the concentration matrix $\hat{\Sigma}_{y,0}^{-1}$ of the present regime, and the factor space in future $\hat{P}_1 \hat{P}_1{}'$.[12] The dimensions of the factor spaces in both windows also need to be estimated during the procedure. Consistent estimations of these objects have been studied extensively. We mainly adopt the estimation procedures proposed in Fan et al. (2013), which provide consistent estimations of the factor space, the concentration matrix, and the idiosyncratic covariance simultaneously. Classical studies Stock and Watson (2002a), Bai and Ng (2002) are also closely related. For a complete exposition, we refer to the original papers.

Recall from the benchmark model in Section 2.1.1 that we have T_j data for regime-j, following

$$\mathbf{y}_{t,j} = \boldsymbol{\chi}_{j,t} + \mathbf{u}_{t,j}, \qquad \text{for } t \in \mathtt{I}_j, \tag{1}$$

where $\Sigma_{\chi,j} = P_j \Lambda_{\chi,j} P_j{}'$ has all nonzero K_j eigenvalues diverging at the rate $O(N)$ (Assumption 1). To optimal access the references mentioned above, we explain the estimation procedures in accordance with the standard specification of the low-rank part $\boldsymbol{\chi}_{j,t}$,

$$\boldsymbol{\chi}_{j,t} = B_j \mathbf{f}_{t,j}, \qquad \text{for } t \in \mathtt{I}_j, \tag{5}$$

where B_j denotes the factor loading matrix fixed within regime for given N, and $\mathbf{f}_{t,j}$ denotes K_j factor signals. By augmenting the T_j data in columns, the data Y_j of the given regime is represented as an N by T_j matrix,

$$Y_j = B_j F_j + U_j, \tag{17}$$

where F_j is a $K_j \times T_j$ matrix of factors and U_j is an $N \times T_j$ matrix of idiosyncratic errors. Under this specification, the benchmark model in Section 2.1.1 can be conditioned on

[12] Recall that this is the projector representation of the factor space $\text{span}(\hat{P}_1)$.

B_j to absorb the linearly growing eigenvalues of $\Sigma_{\chi,j}$, while $\text{var}(\mathbf{f}_{t,j})$ remains finite. The contents of the following Assumptions 6 to 11 closely resemble Assumptions 1 to 4 of Fan et al. (2013), Section 3.

Assumption 6 For each $j \in \{0,1\}$, ${B_j}'B_j/N \to D_j$ as $N \to \infty$ for some full K_j−rank diagonal matrix D_j.

Assumption 7 For each $j \in \{0,1\}$, $(\mathbf{f}_{t,j}, \mathbf{u}_{t,j})$ is stationary, $\mathrm{E}[\mathbf{f}_{t,j}] = \mathrm{E}[\mathbf{u}_{t,j}] = \mathbf{0}$, and $\mathrm{E}[f_{kt}u_{it}] = 0$ for all $i \in \mathcal{N}$ and $k = 1, \ldots, K_j$.

There are additional distributional assumptions on $\mathbf{f}_t$ and $\mathbf{u}_t$: exponential tail behaviors (Assumption 8), a strong mixing condition (Assumption 9), and appropriate moment conditions (Assumption 10). For Assumption 9, denote the $\sigma-$ fields

$$\mathcal{F}_{L_1}^{L_2} \equiv \sigma\big(\{(\mathbf{f}_t, \mathbf{u}_t) \,|\, t \in [L_1, L_2]\}\big)$$

and let the mixing coefficient be

$$\alpha(T) \equiv \sup_{\ell \in \mathbb{Z}} \sup_{A \in \mathcal{F}_{-\infty}^{\ell}, B \in \mathcal{F}_{\ell+T}^{\infty}} \big|\Pr(A \cap B) - \Pr(A)\Pr(B)\big|. \tag{18}$$

Assumption 8 There exist constants $r_1, r_2, b_1, b_2 > 0$ such that for all $j \in \{0,1\}$, for any $s > 0$, $i \in \mathcal{N}$ and $k = 1, \ldots, K_j$,

$$\sup_{t \in \mathtt{I}_j} \Pr(|u_{it,j}| > s) \le \exp\{-s/b_1\}^{r_1},$$
$$\sup_{t \in \mathtt{I}_j} \Pr(|f_{kt,j}| > s) \le \exp\{-s/b_2\}^{r_2}.$$

Assumption 9 There exist $C_r > 0$ and $r_3 > 0$ such that $3r_1^{-1} + (3/2)r_2^{-1} + r_3^{-1} > 1$, satisfying $\alpha(T) < \exp(-C_r T^{r_3})$ for all $T \in \mathbb{Z}_+$.

Assumption 10 There exists $C > 0$ such that, for all $j \in \{0,1\}$, for any $i \in \mathcal{N}$, $s, t \in \mathtt{I}_j$,

(a) $\|\mathbf{b}_{i,j}\|_{max} < C$, for the i−th row vector $\mathbf{b}_{i,j}$ of B_j.

(b) $\mathrm{E}\Big[\big(N^{-1/2}\{\mathbf{u}_{s,j}{}'\mathbf{u}_{t,j} - \mathrm{E}[\mathbf{u}_{s,j}{}'\mathbf{u}_{t,j}]\}\big)^4\Big] < C$,

(c) $\mathrm{E}\big[\|N^{-1/2}B_j'\mathbf{u}_{t,j}\|^4\big] < C$.

Assumption 11 $\ln(N) = o(T^{\gamma/6})$ for $\gamma^{-1} \equiv 3r_1^{-1} + (3/2)r_2^{-1} + r_3^{-1} + 1$, and $T = o(N^2)$.

The assumption of strict stationarity in Fan et al. (2013)(Assumption 2(a)) can be relaxed. The weak stationarity with uniform tail behaviors is sufficient to apply Berstein's inequality in Merlevède, Peligrad, and Rio (2011)(Theorem 1), by which the necessary results in Fan et al. (2013) are produced to guarantee consistency. The strong mixing condition is on the entire time period combining regimes. The rate of N and T is assumed to guarantee consistency, following the original paper.

Under Assumptions 1-2 in Section 2.1.1 and Assumptions 6-11 above, first, the dimension of the factor space in each regime can be consistently estimated following Bai and Ng (2002). A consistent estimate $\hat{K}_j$ of the factor space dimension minimizes the following information criteria

$$IC_{K_j} = \ln V(K_j) + K_j g(N, T_j), \tag{19}$$

where $V(K_j) = \text{tr}(U_j U_j')/NT_j$. The penalty function $g(N,T)$ for any given size (N,T) of the cross-sectional and time dimensions needs to converge to zero slower than the rate $(\min\{N,T\})^{-1}$ (Theorem 2, Bai and Ng (2002)). The same asymptotic property is required by the given regularity conditions based on Fan et al. (2013). We employ the following functions

$$g(N,T) = \frac{N+T}{NT} \ln\Big[\frac{NT}{N+T}\Big] \quad \text{or} \quad g(N,T) = \frac{N+T}{NT} \ln[\min\{N,T\}], \tag{20}$$

introduced in Bai and Ng (2002) and adopted in Fan et al. (2013).

Second, after the consistent estimation of the factor space dimension, the common component $\boldsymbol{\chi}_{j,t}$ is estimated by projecting Y_j on the K_j-leading principal subspace of the sample covariance $\hat{\Sigma}_{y,j}^{\text{sam}} = Y_j Y_j'/T_j$, or on that of the right Gram-matrix $\hat{\Sigma}_{y,j}^{N} = Y_j' Y_j/N$. For $\hat{P}_j = \big[\hat{e}_j^1 | \ldots | \hat{e}_j^{K_j}\big]$, orthonormalized K_j-leading eigenvectors $\{\hat{e}_j^k\}_{k=1,\ldots,K_j}$ of $\hat{\Sigma}_{y,j}^{\text{sam}}$, $\hat{\boldsymbol{\chi}}_j = \hat{P}_j \hat{P}_j' Y_j$ by augmenting the time dimension of $\hat{\boldsymbol{\chi}}_{j,t}$ column-wise. For the cross-sectional dimension $N > T_j$, utilizing K_j-leading eigenvectors $\hat{P}_{T_j}$ of $T_j \times T_j$ matrix $Y_j' Y_j/N$ can be computationally efficient (Stock and Watson (2002a), Bai and Ng (2002)). In this case, $\hat{\boldsymbol{\chi}}_j = Y_j \hat{P}_{T_j} \hat{P}_{T_j}'$. Those are standard and identical methods under the presence of a small number of unobservable factors $K \ll N$.

Third, the factor space information is fully captured by the eigenvectors $\hat{P}_j = \big[\hat{e}_j^1 | \ldots | \hat{e}_j^{K_j}\big]$ of the sample covariance matrix. Note that the estimated common component covariance is $\hat{\Sigma}_{\chi,j} = \hat{\boldsymbol{\chi}}_j \hat{\boldsymbol{\chi}}_j'/T = \hat{P}_j \hat{\Lambda}_{K_j} \hat{P}_j'$, the spectral decomposition of the sample covariance up to K_j regardless of which method estimates $\hat{\boldsymbol{\chi}}_j$ in the second task. The leading K_j- principal subspace $\text{span}(\hat{P}_j)$ of $\hat{\Sigma}_{y,j}^{\text{sam}}$ deviates from $\text{span}(P_j)$ by $o_p(1)$ mainly due to the following reasons: $\|\hat{\Sigma}_{\chi,j} - \Sigma_{\chi,j}\| = o_p(N)$ (due to Lemma 4 of Fan et al. (2013)), the factor prevalence

with the rate $O(N)$ (Assumption 1 of 2.1.1 and Assumption 6), and because the common component covariance $\Sigma_{\chi,j}$ is estimated by $\hat{\Sigma}_{\chi,j}$ of the same rank. We explain in detail the contributions of these terms in Appendix A.

Fourth, Fan et al. (2013) introduced a thresholding method ('POET') to consistently estimate the idiosyncratic covariance under the above set of conditions. The thresholding parameter needs to be gauged with the sparsity parameter $c_{u,j}$ and q_j of $\Sigma_{u,j}$ to secure consistency. Recall from Assumption 2 that $c_{u,j} \equiv \max_{i=1,\dots,N} \sum_{i'=1,\dots,N} |\mathrm{cov}(u_{it,j}, u_{i't,j})|^{q_j} = O(1)$ for some constant $q_j \in [0,1]$. The empirical correlation estimator of $i, i' \in \mathcal{N}$ – the time average of the product of i–th and i'–th residuals $\hat{\mathbf{u}}_{i,j}$ and $\hat{\mathbf{u}}_{i',j}$ – will be adaptively thresholded proportional to

$$\omega_{T,j} \equiv 1/\sqrt{N} + \sqrt{(\ln N)/T_j}, \tag{21}$$

where $c_{u,j}{\omega_{T,j}}^{1-q_j} = o(1)$. Under our simple benchmark assumption $c_{u,j} = O(1)$, it is sufficient to have $\omega_{T,j} = o(1)$ for consistency of the idiosyncratic covariance. Assumptions 9 and 11 assure this rate as $\gamma < 1/2$ and T_j is a fixed portion of the entire T.

Fifth, it is also proven in the same paper that the estimates of idiosyncratic covariance $\hat{\Sigma}_{u,j}$ and the common component covariance estimator $\hat{\Sigma}_{\chi,j} = \hat{\Gamma}_{\chi,j}\hat{\Gamma}_{\chi,j}{}'$ can be plugged into the Sherman-Morrison-Woodbury formula

$$\hat{\Sigma}_{y,j}^{-1} \equiv \hat{\Sigma}_{u,j}^{-1} - \hat{\Sigma}_{u,j}^{-1}\hat{\Gamma}_{\chi,j}\big(I_K + \hat{\Gamma}'_{\chi,j}\hat{\Sigma}_{u,j}^{-1}\hat{\Gamma}_{\chi,j}\big)^{-1}\hat{\Gamma}'_{\chi,j}\hat{\Sigma}_{u,j}^{-1}, \tag{22}$$

where $\hat{\Gamma}_{\chi,j} = \hat{P}_j\hat{\Lambda}_{K_j}^{1/2}$, to give a consistent estimation of the concentration matrix of $\mathbf{y}_{t,j}$. The rate $\|\hat{\Sigma}_{y,j}^{-1} - \Sigma_{y,j}^{-1}\| = \|\hat{\Sigma}_{u,j} - \Sigma_{u,j}\| = O_p({c_{u,j}\omega_{T,j}}^{1-q})$.

Finally, the number of granular units $H \equiv \mathrm{rank}(W)$ for $W \equiv P_0^{\perp}P_0^{\perp\prime}P_1P_1{}'$ can be decided by the number of nonzero eigenvalues of its sample analogue

$$\hat{W} \equiv \hat{P}_0^{\perp}\hat{P}_0^{\perp\prime}\hat{P}_1\hat{P}_1.$$

Although numerous sophisticated methods can be applied, in applications, a check on the eigenvalue gap through the scree plot of the matrix $\hat{W}$ will be the most uncomplicated yet acceptable procedure.

Ranking Consistency of the Influence Measure

The proposed measure $\mathcal{I}_i \equiv \left\|\Sigma_{y,0}^{-1}P_1P_1{}'\Sigma_{y,0}^{-1}\boldsymbol{\sigma}_{u,0}^{i}\right\|$ is a norm of each column of

$$\mathcal{I} \equiv \Sigma_{y,0}^{-1}P_1P_1{}'\Sigma_{y,0}^{-1}\Sigma_{u,0}. \tag{23}$$

The membership detection based on ranking $\{\mathcal{I}_i\}_{i\in\mathcal{N}}$ can be proven to be valid by showing consistency of the ranking of $\{\hat{\mathcal{I}}_i\}_{i\in\mathcal{N}}$ between the granular and the non-granular units.

The consistency can be proven in a similar way as in Brownlees and Mesters (2021), exploiting the consistency of $\mathcal{I}$ estimation.
Define event Υ, where the estimated influence measures are indeed higher for the granular units than those for the non-granular units, that is,

$$\Upsilon \equiv \left\{ \|\hat{\mathcal{I}}_g\| > \|\hat{\mathcal{I}}_i\| \,|\, g \in \mathcal{G}, i \in \mathcal{G}^c \right\}. \tag{24}$$

Proposition 2. Under the Assumptions 1-2 in 2.1.1 and 6-11, event Υ holds asymptotically almost surely.

The proof is left to Appendix A.

4.2 Detection of Structural Breakpoints

We now propose a new method to estimate single or multiple breakpoints of the factor space change based on the distance measure (10), the square of the projector metric. Our approach introduces an information criterion that integrates two types of model selection – one for determining the presence of a breakpoint and another for identifying the location of a breakpoint.

Let us first consider cases where there is potentially one breakpoint in any time domain of interest, $\mathtt{I}$, of length T. A model with breakpoint will take a point $t(\tau) = \lfloor \tau T \rfloor \in \mathtt{I}$ for some $\tau \in (0,1)$ and assume that there are distinct factor spaces before ($\mathtt{I}_0(\tau)$) and after ($\mathtt{I}_1(\tau)$) the point, respectively. Denote $\hat{\mathcal{P}}_j(\tau)$ the estimated factor space from the window $\mathtt{I}_j(\tau)$.

The sample analogue $\hat{d}(\tau) = \mathrm{tr}[\hat{\mathcal{P}}_0{}^{\perp}(\tau)\hat{\mathcal{P}}_1(\tau)]$ measures the information gain by introducing a 'new' regime after $t(\tau)$. This gain should be penalized by complexity of the model by having two regimes before and after $t(\tau)$. Recall that the factor space $\mathcal{P}_j(\tau)$ is estimated by minimizing $\mathrm{tr}[\hat{\Sigma}^{\mathrm{sam}}_{u,j}(\tau)]$ in each supposed regime $\mathtt{I}_j(\tau)$ by following the information criteria (19) of Bai and Ng (2002). Denote T_j the length of the window $\mathtt{I}_j(\tau)$. The optimized penalty term of the information criteria of Bai and Ng (2002),

$$g_j \equiv \hat{K}_j \frac{N + T_j}{NT_j} \ln\left(\frac{NT_j}{N + T_j}\right), \tag{25}$$

which solves the optimal factor space $\hat{\mathcal{P}}_j(\tau)$, captures the complexity of having one factor model (1) in each supposed regime $\mathtt{I}_j(\tau)$. Hence, we propose the combined penalties,

$$G(\tau; 1) = G\big(\{N, T_j, K_j\}_{j \in \mathcal{J}}\big) = g_0 + g_1, \tag{26}$$

to construct total information gain for having one break at $t(\tau)$ as follows.

$$S(\tau;1) \equiv \ln \mathrm{tr}\big[\hat{\mathcal{P}}_0^{\perp}(\tau)\hat{\mathcal{P}}_1(\tau)\big] - G(\tau;1). \tag{27}$$

The statistic for the model without breakpoint will be formulated by

$$S(0) \equiv -G(0), \tag{28}$$

where $G(0)$ denotes the optimized penalty term that fits one approximate factor model for the entire window `I`, such that

$$G(0) \equiv \hat{K}\frac{N+T}{NT}\ln\left(\frac{NT}{N+T}\right).$$

To have a breakpoint at $b = \tau^* T$ for certain $\tau^* \in (0,1)$, the information gain $\hat{d}(\tau^*) = \mathrm{tr}[\hat{\mathcal{P}}_0{}^{\perp}(\tau^*)\hat{\mathcal{P}}_1(\tau^*)]$ should be sufficiently large to favor the existence of two distinct regimes within `I`. That is, we require

$$S(\tau^*;1) > S(0). \tag{29}$$

Conditional on the existence of a breakpoint, the location of the break τ^* is chosen by maximizing the penalized information gain, such that

$$\tau^* = \mathrm{argmax}_{\tau\in(0,1)} S(\tau;1).$$

As $S(\tau^*;1)$ is the maximum value, to conclude there is no breakpoint in `I`, it is enough to check whether

$$S(\tau^*;1) < S(0). \tag{30}$$

The case of multiple breakpoints can be broken down into a task finding sub-windows with a single breakpoint. First, find a breakpoint $b_{1,0}$ in the whole window (`I`) of length T and find the next breakpoint in a window starting from the updated initial point after the first breakpoint. If there is a second breakpoint $b_{2,0}$ in this window, the first breakpoint should be the single breakpoint in the subwindow $[1, b_{2,0}]$. More precisely, if

$$S(b_{1,0};1)\big|_{[1,b_{2,0}]} < S(0)\big|_{[1,b_{2,0}]}\big(= -G(0)\big|_{[1,b_{2,0}]}\big),$$

either $[1, b_{2,0}]$ does not have a breakpoint or its breakpoint should be updated from $b_{1,0}$. If it is updated to $b_{1,1}$, the $b_{2,0}$ should be a breakpoint in the remaining window $[b_{1,1}, T]$ as well. This property should be satisfied by all subsequent breakpoints.

5 Simulations

This section contains two simulations: one for granular unit detection (in the first subsection, following discussions in Section 3.3.1 and 4.1), and another for structural breakpoint estimation (in the second subsection, following discussion in Section 4.2). The simulation for granular unit detection presents higher success rates in identifying true granular groups as those with larger gaps in their systemic influence relative to non-granular units. The results for breakpoint estimation indicate higher performance in detecting the correct number of breakpoints at precise locations in scenarios with stronger factor structures and longer time windows for each regime.

5.1 The Detection of the Granular Units

Consider a system of $N = 100$ cross-sectional units in two regimes ($J = 2$). Each regime ($j = 0, 1$) has $T_j = 100$ data, both with $K = 3$ dimension of the factor space. Assume that the breakpoint at $T_1 = 100$ is known.

The regime change amounts to a change of factor space $\text{span}(P_0)$ to $\text{span}(P_1)$. P_0 is a randomly chosen orthonormal $N \times K$ matrix whose column space equals the regime-0 factor space $\text{span}(P_0)$. We assume $\mathbf{f}_t \sim \mathcal{N}(\mathbf{0}_{K\times 1}, \Sigma_\chi = \sigma_\chi^2 I_K)$ and loaded by P_0 during the first regime, and $\mathbf{u}_t \sim \mathcal{N}(\mathbf{0}_{N\times 1}, \Sigma_u = \sigma_u^2 I_N)$. It is further assumed that Σ_χ and Σ_u are fixed across regimes, with $\sigma_\chi = 5$ and $\sigma_u = \sqrt{2}$. That is, for any $j \in \{0, 1\}$,

$$\mathbf{y}_t = P_j \mathbf{f}_t + \mathbf{u}_t \quad \text{for} \quad t \in \mathtt{I}_j.$$

The regime-1 factor space basis P_1 is chosen so that combined with $\Sigma_{y,0}^{-1}$, the resulting $\text{span}(P_1)$ implies a particular set $\mathcal{G}$ of three units as the set of granular units based on the measure $\mathcal{I}_i \equiv \left\| \Sigma_{y,0}^{-1} P_1 P_1' \Sigma_{y,0}^{-1} \boldsymbol{\sigma}_{u,0}^i \right\|$ in equation (13). We present 48 different sets $\mathcal{G}$ of granular units (and the corresponding choices of P_1), while keeping the distance $d\big(\text{span}(P_0), \text{span}(P_1)\big) \equiv \text{tr}\big[\mathcal{P}_0^\perp \mathcal{P}_1\big]$ in (10) the same. Distinct choices of the P_1 point in various directions and span different three-dimensional subspaces within the entire $N = 100$ dimension. The different factor space dynamics – and the corresponding groups $\mathcal{G}$ or $\text{span}(P_1)$ – present different influence gaps between the granular units and the non-granular units. The groups are numbered by their rankings of the influence gap measured as the ratio of $\mathcal{I}_H$ and $\mathcal{I}_{H+1}$ in descending order.

Let us detail the construction of the sample granular groups. The collection is first randomly chosen among the groups with the influence gap ($\equiv \mathcal{I}_H / \mathcal{I}_{H+1}$) in the range $(1.10, 2.03)$ and the average group influence $\bar{\mathcal{I}}_\mathcal{G} \equiv (\sum_{g=1}^H \mathcal{I}_g)/H > 0.1$. By the design of the influence measure, some units can appear much more frequently in many different

groups than other units. As discussed in Section 3.2, the units that have a relatively high centrality in regime-0 based on $\Sigma_{y,0}^{-1}$ can appear as granular units in many different scenarios of factor space change; such as, for example, the units $(65, 64, 47)$ that are the top 3 of the highest column norms of $\Sigma_{y,0}^{-1}$ by 2-norm. Besides, due to the homogeneous and diagonal Σ_u in our setup, those who have more intense loads of the change $P_1 P_1{}'$ from $P_0 P_0{}'$ will also appear as granular units, for example, the indices $(1, 22, 63)$.[13] The group collection has been adjusted to encompass more than half of all 100 units in the group membership. The membership list of the 48 different groups is presented in Table 1 below.

Group Identities by $\mathcal{I}_H/\mathcal{I}_{H+1}$ ranking							
1	[43 92 13]	13	[43 63 96]	25	[21 63 18]	37	[22 55 3]
2	[79 65 1]	14	[100 90 29]	26	[79 65 5]	38	[7 65 84]
3	[47 57 1]	15	[22 77 64]	27	[12 57 29]	39	[63 57 62]
4	[77 47 42]	16	[59 81 65]	28	[47 77 96]	40	[63 21 90]
5	[68 73 69]	17	[73 88 68]	29	[47 17 96]	41	[9 10 90]
6	[22 65 25]	18	[99 85 1]	30	[13 22 81]	42	[63 62 55]
7	[22 88 59]	19	[21 17 7]	31	[1 57 16]	43	[6 29 8]
8	[23 63 66]	20	[45 57 16]	32	[17 45 16]	44	[13 73 20]
9	[79 45 59]	21	[79 88 5]	33	[69 67 64]	45	[10 12 9]
10	[79 77 11]	22	[1 9 6]	34	[23 7 20]	46	[56 11 60]
11	[23 44 5]	23	[56 7 60]	35	[13 7 81]	47	[11 36 5]
12	[42 69 1]	24	[92 47 5]	36	[22 75 25]	48	[6 69 59]

Table 1: Sample collection of granular groups

The sample analogue $\hat{\mathcal{I}}_i = \left\| \hat{\Sigma}_{y,0}^{-1} \hat{P}_1 \hat{P}_1{}' \hat{\Sigma}_{y,0}^{-1} \hat{\boldsymbol{\sigma}}_{u,0}^i \right\|$ is constructed following the estimation methods discussed in Section 4.1. We repeat the process $M = 500$ times for each $\mathcal{G}$ and count the number of successful detection of the true membership of $\mathcal{G}$. A detection is considered successful only when it detects all three members correctly, while correct detection of only some of the members of $\mathcal{G}$ is considered a failure. The random seeds for the draws of $\mathbf{f}$ and $\mathbf{u}$ are the same across the different sets of true granular units.
Figure 2 presents the results of this simulation exercise.

[13] That is, the indices corresponding to the columns $P_1 P_1{}' - P_0 P_0{}'$ of relatively high vector norms.

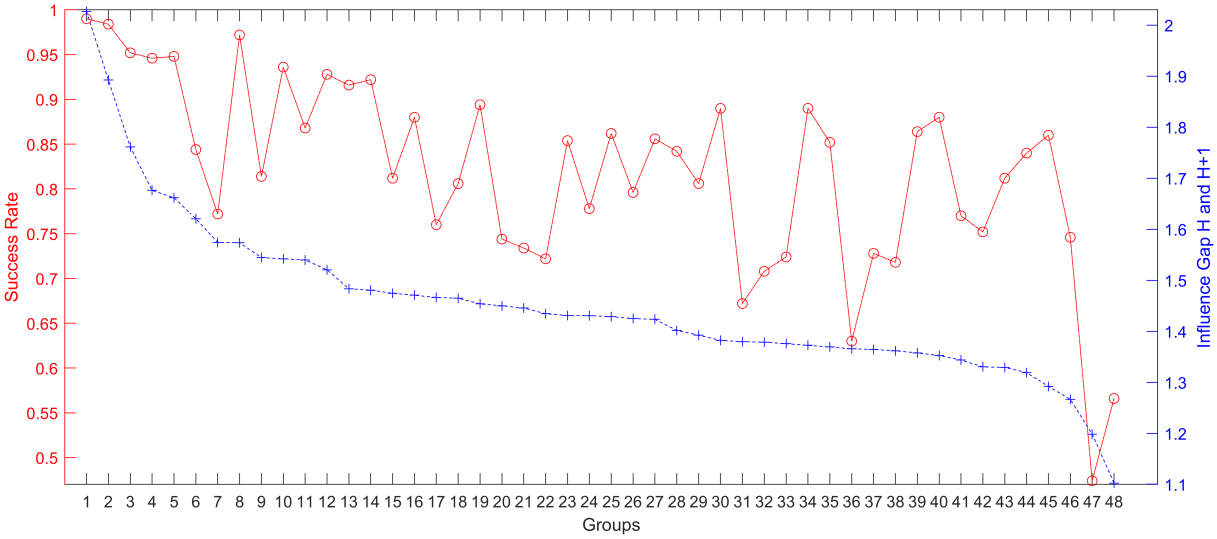

Figure 2: Success Rate of the Granular Unit Detection
(by the influence Gap, $\mathcal{I}_H/\mathcal{I}_{H+1}$)

The rate of successful detection overall presents the anticipated decreasing trend as the influence of the granular units becomes less distinguished compared to non-granular units. In this trial, if the least essential granular unit is still 40% more influential than the non-granular units, the rate of successful detection of the granular units is higher than 72.2%. The average group influence $\bar{\mathcal{I}}_G \equiv (\sum_{g=1}^{H} \mathcal{I}_g)/H$ does explain some fluctuations. For example, groups [22 88 59] and [79 45 59] show the earliest drops in success rate while being in ranking 7 and 9 by the influence gap ($\mathcal{I}_H/\mathcal{I}_{H+1}$), respectively. Those groups only come as the ranking 29th and the 45th in terms of the average group influence. On the contrary, groups [63 21 90] and [10 20 19] that show the latest peaks in ranking the 40th and the 45th by the influence gap will come earlier as the 15th and the 26th by the ranking of the average group influence ($\bar{\mathcal{I}}_G$). A relatively strong systemic influence exerted collectively by the granular units contributes to improved detection performance.

5.2 Structural Breakpoints

We present the results of the detection of single (in the first subsection) or double breakpoints (in the second subsection) based on the detection criteria in Section 4.2. The total length of time periods is denoted as $T = \sum_j T_j$, the sum of the length of all supposed regimes T_j. The cross-sectional dimension is fixed to $N = 100$ in any regime. Each regime has $K = 3$ dimension of the factor space. We assume again that $\mathbf{f}_t \sim \mathcal{N}(\mathbf{0}_{K\times 1}, \sigma_f^2 I_K)$, loaded by P_0 during the first regime, and $\mathbf{u}_t \sim \mathcal{N}(\mathbf{0}_{N\times 1}, \sigma_u^2 I_N)$. In the following, we fix $\sigma_u^2 = 2$ and vary σ_f^2. The seeds of the random signal draw are fixed overall 500 trials. The underlying sequence of the factor spaces is fixed as well. span(P_0), span(P_1) and

span(P_2) are constructed from a randomly chosen orthonormal $N \times K_0$ matrix P_0 fixing the distances between two subsequent factor spaces, based on the distance measure (10). The caption numbers of the figures in this section indicate the corresponding scenarios they represent.

5.2.1 Single Breakpoints

We first present how the maximization of the statistics (27) performs in the case of single breakpoints in various relative locations, accompanied by the criteria of existence of a breakpoint (29). We inspect the stride-1 grid in the window of inspection that consists of 20-time points before and after the true location of the breakpoint('BP'), $[BP - 20, BP + 20]$.
The following relative locations of the breakpoint are considered:

(a) A breakpoint located central at $BP = 100$, with $T_0 = 100$ and $T_1 = 100$ before and after the break.

(b) A central breakpoint $BP = 50$, with shorter time spans before and after the break, $T_0 = 50$ and $T_1 = 50$, than the case (a).

(c) A breakpoint located on the left side of the entire time window (T) at $BP = 50$, with a shorter time span before ($T_0 = 50$) than after ($T_1 = 100$) the break.

(d) A breakpoint located on the right side of the entire time window (T) at $BP = 100$, with a shorter time span after ($T_1 = 50$) than before ($T_0 = 100$) the break.

The table below shows the number of trials that correctly conclude a single breakpoint at the exact location out of 500 entire number of trials. The inspected range of the relative intensity of the factor signals $SN \equiv \sigma_f^2/\sigma_u^2$ is from 10 to 30. In the application on the high dimensional data, we found the relative strength of the factor signals easily go over 10 for regimes before and after the systematic breakpoints of our interests.

$SN = \sigma_f^2/\sigma_u^2$	10	12.5	15	17.5	20	22.5	25	27.5	30
(a) BP = 100, center	37.8	75.2	85	88.2	90.8	93	93.4	94.2	95
(b) BP = 50, center	5.6	15.8	34.2	54.8	70.2	78.4	84	86.4	88
(c) BP = 50, left	14	20.8	36.6	53.6	66	76.4	81.8	85.2	86.6
(d) BP = 100, right	14	42.6	63.2	72.2	78	79.4	81.6	83.4	84.8

Table 2: The rate of concluding single BP at the exact location
(%, out of 500 trials)

The results for the central breakpoints (a) and (b) in Table 2 suggest that the detection scheme will successfully detect a breakpoint by a higher probability when there is a longer duration of the time window before and after the breakpoint. The detection criteria conclude the single breakpoint at the exact location for 75% of the trials with relatively less intense factor signals ($SN = 12.5$) for scenario (a), where the durations of the before and after regimes are comparable to the size of the cross-section $N = 100$ as shown in Figure 3.

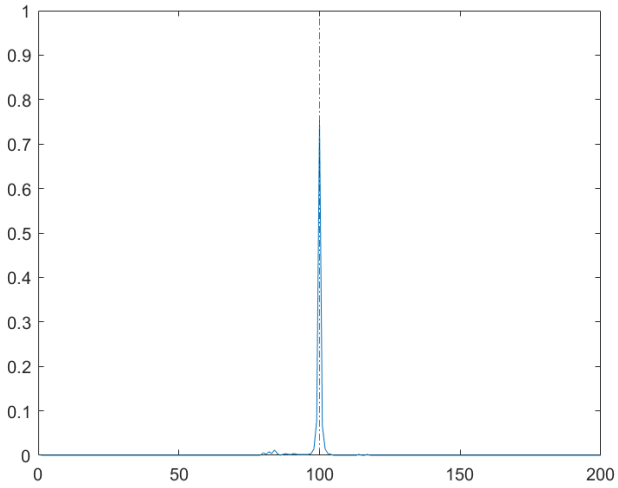

Figure 3: (a) $BP = 100$, $T_0 = T_1 = 100$ ($SN = 12.5$).

The examples for SN over 20 in Figure 4 and 5 indicate the performance of the detection for the various scenarios. Especially, when the durations of two regimes are asymmetric, having a shorter time span after a break (scenario (d)) performs better than having a shorter time span before a break (scenario (c)) for cases of low or moderate relative signal strength of the factors (SN). Given the lengths of the subsequent regimes, the results for varying SN for all scenarios indicate that the performance of the detection of a single breakpoint will be improved under the presence of the factor signals sufficiently intense.

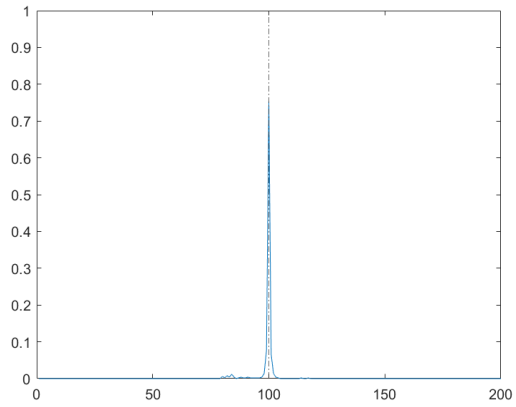

(a) $BP = 100$, $T_0 = T_1 = 100$.

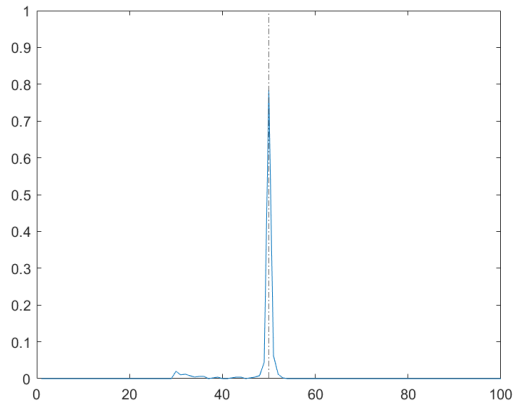

(b) $BP = 50$, $T_0 = T_1 = 50$.

Figure 4: Central Breakpoints, $SN = 22.5$.

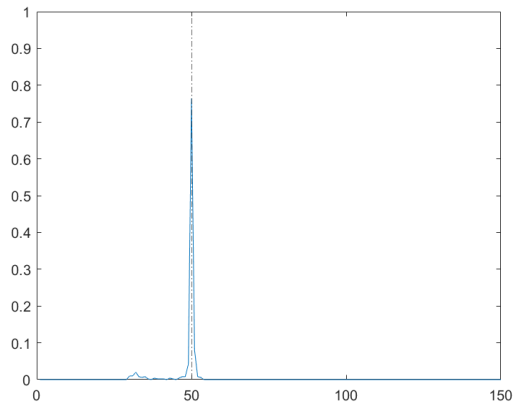

(c) $BP = 50$, $T_0 = 50$, $T_1 = 100$.

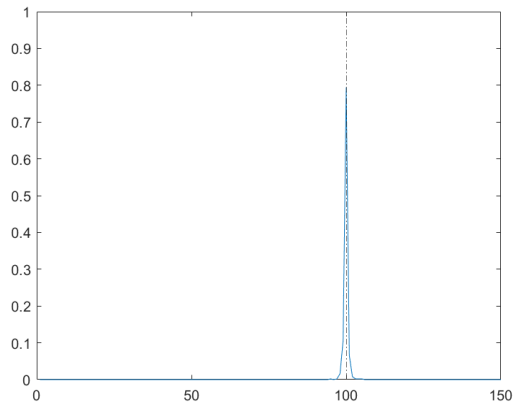

(d) $BP = 100$, $T_0 = 100$, $T_1 = 50$.

Figure 5: Side Breakpoints, $SN = 22.5$.

5.2.2 Multiple Breakpoints

Now, let us discuss the result of the detection of multiple breakpoints. Consider two breakpoints with different time spans before and after as the following scenarios,

(A) $BP_1 = 70$ and $BP_2 = 140$ in the entire time window of length $T = 210$.

(B) $BP_1 = 50$ and $BP_2 = 100$ in the entire time window of length $T = 150$.

Again, the finest grid with stride 1 will be inspected, yet without restricting the window of inspection in a neighborhood of the true breakpoints. The inspection covers the whole window except the first and last 20 time points, which is less than 15%–grid size of the

shortest entire window length $T = 150$ of the scenario (B). For each scenario, the detection proceeds to find maximum 5 breakpoints.

Table 3 below shows the number of detections across 500 trials counted as success by satisfying the following criteria. First, it should conclude the existence of the correct number of breakpoints, two. Second, the estimated breakpoints concluded as either the first (out of two breakpoints) or the second (out of two breakpoints) are located within the neighborhood $[BP_\iota - a, BP_\iota + a]$ of the true breakpoint BP_ι of radius a, which is 10% of the duration of one regime; $a = 5$ in case (A) and $a = 7$ in case (B). The success rate is reported separately for each breakpoint and jointly as well. We present the range of the SN from over 10 to over 30 in the following table. The existence of multiple breakpoints undermines the performance of the detection for relatively low SN. For example, in case (A) with a shorter window size, the success rate of locating the first or second BP in the target neighborhood is less than 1% when $SN = 10$.

$SN = \sigma_f^2/\sigma_u^2$			12.5	15	17.5	20	22.5	25	27.5	30	32.5
(A)	$(BP_1, BP_2) = (50, 100)$	BP_1	2.4	5.6	8.6	16.8	31.2	45	59.2	75.4	84.2
		BP_2	5.6	7.4	16.2	27.8	45.4	55.6	65.2	77.6	80.4
		Joint	1	1.4	5.8	14.4	28.8	43.2	56.6	70.6	76.4
(B)	$(BP_1, BP_2) = (70, 140)$	BP_1	4.8	4.4	11.4	18.4	40.2	61.4	73	85.4	92.8
		BP_2	3.2	5.8	15.8	29.2	50.4	67.6	77	85.8	88.6
		Joint	1	1.6	7.6	16.2	37.8	59.4	70.2	82.6	87.2

Table 3: Success rate of detecting two BPs located in the target neighborhoods
(%, out of 500 trials)

The correct detection rates are higher in case (B), which features a longer duration of subsequent regimes. The success rate for case (B) is still higher when we narrow down the target neighborhood as the same as case (A). Figure 6 give a comparison of the success rates calculated separately for two breakpoints.

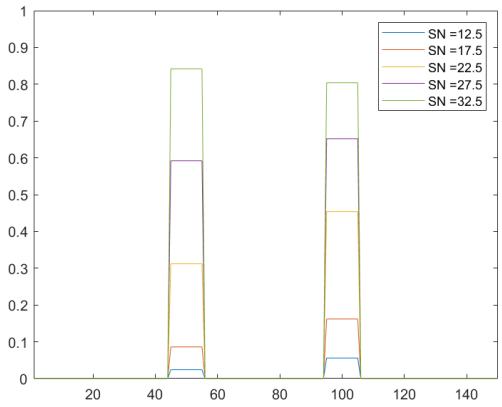

(A) $(BP_1, BP_2) = (50, 100)$, $T = 150$.

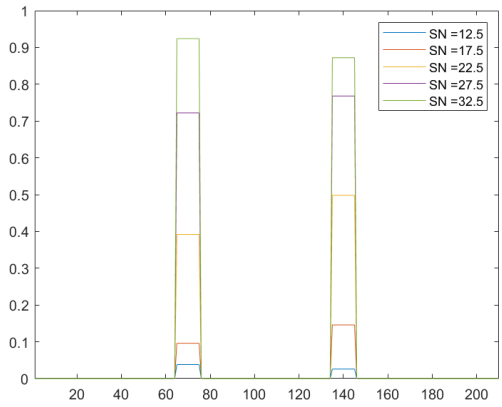

(B) $(BP_1, BP_2) = (70, 140)$, $T = 210$.

Figure 6: Success rates for the target neighborhoods of radius 5 (separately for each BP)

The success rates of detecting two breakpoints jointly within the target neighborhoods are shown in Figure 7. The results show an improved performance of the joint detection where there is a strong enough factor structure within each regime.

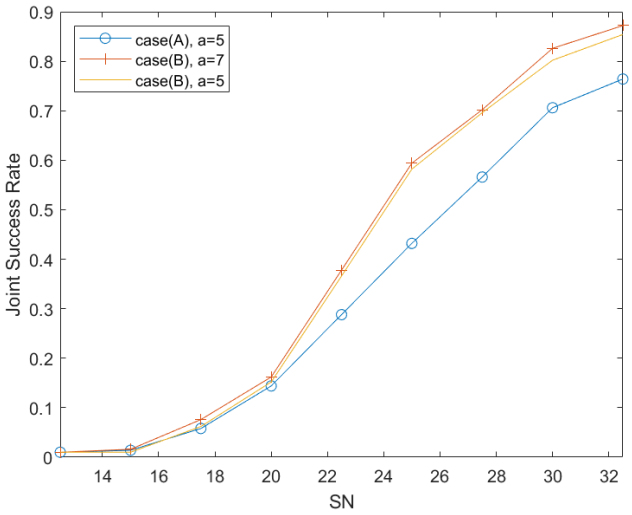

Figure 7: Joint Success Rates

6 Applications

As long as there is reasonable information about a structural break, our method can be applied to screen for potential key players governing the dynamics of the second-moment structure of the system. We apply the proposed detection scheme for granular units from Section 3.3.1 and the breakpoint estimation method from Section 4.2 to a panel of the daily

S&P 100 return (log price differences), utilizing the data shared in Barigozzi and Hallin (2017).[14] The data contains daily closing prices of $N = 90$ constituents of S&P 100 index traded from the period January 03, 2000 to September 30, 2013. We focus our analysis on the historical periods of the dot-com bubble burst (2000-2001) and the global financial crisis (2007-2008). The proposed granular detection scheme finds reasonable potential key actors from the early stages of the crisis, featuring our own breakpoint estimation. The results will be discussed as well for an extended panel, which also includes notable companies that were delisted during or shortly after each crisis period. Especially for the period 2007-2008, the inclusion of the missing units substantially affects the breakpoint and, hence, the result of the granular unit detection.

Two studies provide reference points for comparison regarding granular unit detections and structural break dates. For structural breakpoints, we reference the common component breakpoint dates in Barigozzi et al. (2018) ('BCF2018') to compare with our estimated breakpoint dates. BCF2018 studied breakpoint estimation of the common and idiosyncratic components and applied the method to daily S&P 100 return data (differences of the log daily closing prices) of $N = 88$ stocks traded from January 04, 2000, to August 10, 2016. We assume that the result of the common component breakpoints for the periods of interest (the years 2000 - 2001 and 2007 - 2008) in BCF2018 are not affected by minor differences in the datasets due to the potential delisting of constituents during the period from September 30, 2013, to August 10, 2016.[15] Breakpoints estimated using our method utilizing the data Barigozzi and Hallin (2017) show overall similarity with the common component breakpoints reported in BCF2018.

For granular unit detection, the method of Brownlees and Mesters (2021) will be the benchmark. The comparison will focus on membership detection. Let us recall the granular unit detection criteria in Section 3.3.1:

Detection of the set of Granular units (Section 3.3.1) The set $\hat{\mathcal{G}}$ of granular units consists of $\hat{H} = \text{rank}(\hat{\mathcal{P}}_0^{\perp}\hat{\mathcal{P}}_1)$ cross-sectional units with the highest column norms,

$$\hat{\mathcal{I}}_i = \left\| \hat{\Sigma}_{y,0}^{-1} \hat{P}_1 \hat{P}_1{}' \hat{\Sigma}_{y,0}^{-1} \hat{\boldsymbol{\sigma}}_{u,0}^{i} \right\|.$$

[14] The data can be retrieved at http://wileyonlinelibrary.com/journal/rss-datasets.

[15] From S&P 500 constituent list – the historical S&P 100 constituent list is licensed and was not available – in CRSP data (through WRDS), we found only DELL was delisted among the 90 stocks of Barigozzi and Hallin (2017) during the period from September 30, 2013, to August 10, 2016.

The benchmark reference for membership detection (Brownlees and Mesters (2021)) is based on the $\hat{H}$−highest column norms $\|[\hat{\Sigma}_y^{-1}]^i]\|$,[16], analyzed for both separate and combined regimes. The construction of the measures $\hat{\mathcal{I}}_i$ and $\|[\hat{\Sigma}_{y,j}^{-1}]^i]\|$ follows the procedure described in Section 4.1. For breakpoints provided by Barigozzi et al. (2018) or estimated using our methods, the granular units detected through our proposed method are better interpreted as the potential key sources within the historical context of each crisis.

6.1 Dot-Com Bubble

Figure 8 below summarizes the results of the granular unit detection based on the proposed criteria 3.3.1, applied to breakpoints obtained from our own estimations (indicated in blue) and from BCF2018 (indicated in black).

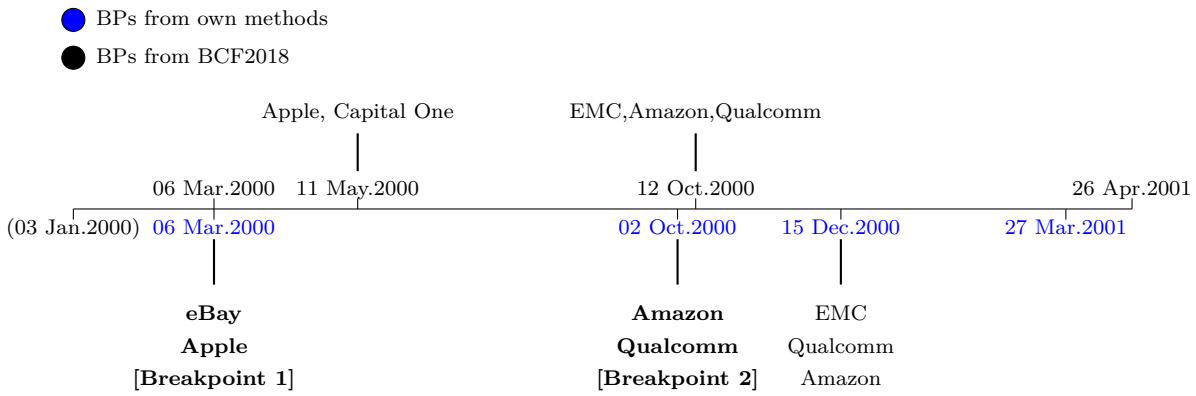

Figure 8: Granular Units in Dot-com bubble, based on $\hat{\mathcal{I}}_i$

Overall, the detected granular units based on the estimated influence measure $\hat{\mathcal{I}}_i$ are major players in e-commerce (eBay or Amazon) or big tech companies (Apple, Qualcomm, EMC), which are the reasonable key contributors in the onset of the dot-com bubble burst. The identity of the detected granular units is not highly sensitive to the length of the post-break window. For instance, for the first breakpoint, eBay remains the top granular unit even when the post-break window is reduced to 20 days or shorter.

For comparison, the results based on the concentration matrix for the windows before and after breakpoints 1 and 2 are presented in Table 4.

[16] $[\hat{\Sigma}_y^{-1}]^i$ denotes the i−th column of $\hat{\Sigma}_y^{-1}$.

$\mathtt{I}_0$: Jan 3, 2000 - Mar 6	$\mathtt{I}_1$: Mar 7 - Oct 2, 2000	$\mathtt{I}_2$: Oct 3 - Dec 15, 2001
Simons Property Group	ExxonMobil	Simons Property Group
General Electric	Chevron	Citigroup

Table 4: Granular Units in Dot-com bubble, based on $\|[\hat{\Sigma}_{y,j}^{-1}]^i]\|$

When combining $\mathtt{I}_0$ and $\mathtt{I}_1$ ($\mathtt{I}_0 \cup \mathtt{I}_1$) or $\mathtt{I}_1$ and $\mathtt{I}_2$ ($\mathtt{I}_1 \cup \mathtt{I}_2$), the granular units identified include companies in the energy sector, such as ExxonMobil, Chevron, and ConocoPhillips. For the windows before and after the latest breakpoint (December 15), companies in similar sectors—industrial, finance, or energy—were also identified, as shown in the earlier windows presented in Table 4.

For the period surrounding the dot-com crash, the breakpoints and detected granular units do not change substantially when adding notable missing entities like Enron, Yahoo, WorldCom, or Global Crossing to the panel. The most significant change occurs at the first breakpoint (March 6), which shifts 10 days earlier; however, eBay remains the top granular unit.

6.2 2007-2008 Financial Crisis

The proposed granular unit detection identified all financial companies as the granular units at the given or estimated breakpoints. Our breakpoint estimation method detected a breakpoint in September 2008, coinciding with the historical peak of the global financial crisis, which aligns with the result reported in BCF2018. The granular units at the September breakpoint are nearly identical across both sets of dates. In addition, our own estimation points to an earlier breakpoint in July 2008, which identified another set of notable financial institutions—Bank of America, Wells Fargo, and AIG—as the granular units.

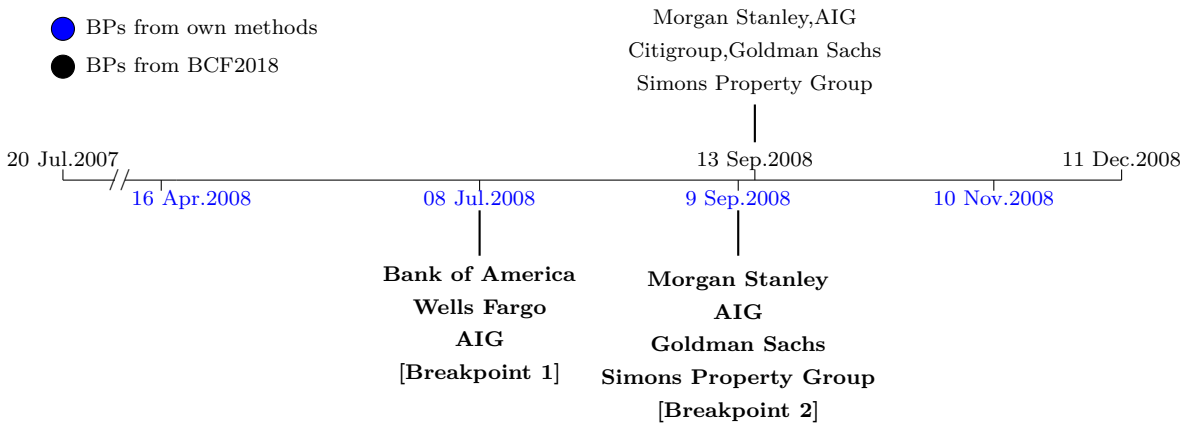

Figure 9: Granular Units in 2008 Financial Crisis, based on $\hat{\mathcal{I}}_i$

The concentration matrix identifies companies in various sectors as granular units, as shown below for the top three granular units (the year '2008' is omitted in the first row of Table 4). The sectors are spread across healthcare, utilities, consumer discretionary, and energy for the separate windows. For the combined windows, the industrial and telecommunications sectors are also included.

$\mathtt{I}_0$: Apr 16 - Jul 7	$\mathtt{I}_1$: Jul 8 - Sep 8	$\mathtt{I}_2$: Sep 9 - Nov 10
Johnson & Johnson	Allstate	McDonald's
Baxter	Eli Lilly and Company	The Walt Disney Company
Southern Company	Johnson & Johnson	Chevron

Table 5: Granular Units in the Global Financial Crisis, based on $\|[\hat{\Sigma}_{y,j}^{-1}]^i]\|$

Although the proposed granular unit detection captures relevant units in the context of the financial crisis, the estimated (or given) breakpoints are too late to provide practical insights into potential systemic risk. During the global financial crisis, the major correlation structure—with or without notable units such as Lehman Brothers, Bear Stearns, Merrill Lynch, Washington Mutual, and General Motors—shows a substantial difference. Figure 10 below presents the results of the breakpoints and corresponding granular units for the panel extended in the cross-sectional dimension to $N = 95$, covering the period from January 3, 2007, to May 30, 2008. Note that Bear Stearns was delisted after May 30, 2008.

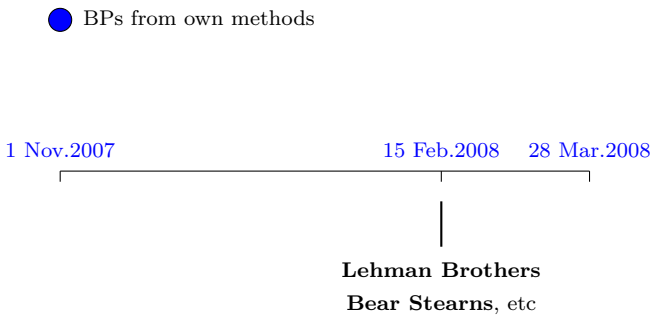

Figure 10: Granular Units in Early 2008, based on $\hat{\mathcal{I}}_i$

The breakpoints occurred in November 2007, as well as in February and March 2008. The breakpoint on February 15, which occurred earlier than any major collapse, highlights Lehman Brothers and Bear Stearns—whose later collapses (Bear Stearns on March 16, 2008, and Lehman Brothers on September 15, 2008) preluded and triggered the most significant events in the financial crisis—as the top two granular units. Washington Mutual, the parent company of the largest savings and loan association, Washington Mutual Bank, which collapsed in September 2008, was already identified as the top granular unit at the earlier November 1, 2007 breakpoint. The identity of the granular units remains stable even when the length of the post-break data is reduced or when there are slight changes in the breakpoint itself. Although the factor space estimation becomes noisy, Lehman Brothers and Bear Stearns remain the top granular units, even when the post-break window is shortened to less than 20 days.

The membership detection is based on the collective feature of systemic influence discussed in Section 3.2. The detected granular units do not necessarily exhibit the largest changes in their idiosyncratic volatility or correlations with other units. For the dot-com bubble breaks, nearly all of the detected granular units are far outside the Top 10 for idiosyncratic covariance change before and after the considered breaks, based on the column norm. Only Apple was within the Top 10, as it was ranked 9th. In the case of the financial crisis, Bank of America, AIG, and Morgan Stanley are outside the Top 10, and none of the detected granular units are within the Top 3. The chosen granular units are not necessarily those that had the highest loadings of the common factors after the break, either. For instance, after the break during the dot-com crash, common factors loaded more heavily on Texas Instruments than on Qualcomm. Similarly, during the financial crisis, companies in the Energy (e.g., NOV, APC, OXY) or Materials (e.g., FCX) sectors had higher loadings than Goldman Sachs or Simon Property Group.

We found that, through this application, the proposed criteria and influence measure effectively capture reasonable potential sources of the known crises. Our method can

be seen as providing a fairly conservative measure of systemic influence. By identifying individual-level effects during considerable systemic breaks, our approach minimizes the debate about whether the influence of certain individuals is truly system-wide. Furthermore, while the detection scheme is feasible after a break has occurred, the results show that the proposed method provides prompt information about probable risk components at the early stages of each crisis.

Note that the assumption of a stationary factor structure underlying the concentration matrix-based measure becomes less plausible in a high-frequency data environment. A more appropriate comparison could be made with detection methods that model the dynamics of correlations, such as those described in Basu and Rao (2021) using a network model. However, our approach retains the advantage of simplicity compared to methods that involve the explicit modeling of a dynamic network of correlations.

7 Concluding Remarks

We propose a novel detection scheme for identifying potential systemic risk components by estimating and utilizing structural breaks in panel data. Our method offers a straightforward approach for analyzing the impact of idiosyncratic second moments on system-wide second moments. Compared to other approaches that address correlation dynamics, our method is simpler and relies on the well-established theory of factor models and principal component analysis (PCA). Additionally, we provide insights into interpreting the latent factor model as a network model. Applied to daily stock return data, our scheme successfully identified plausible sources of well-known economic crises at relatively early stages, demonstrating its potential for real-time application.

The proposed granular unit detection scheme has extended applicability. While this paper interprets cross-sectional units as individual entities (such as firms or banks), in principle, the units can represent any collection of time-varying variables. For example, by including both real and financial variables, the detection scheme could identify which types of variables contribute most to system-wide instabilities.

Another potential extension relates to the literature on granular instrumental variables (IV). In Gabaix and Koijen (2021), the optimal weighting of idiosyncratic shocks for constructing granular IV is orthogonal to the factor loading. As discussed in Appendix E, these orthogonal directions in the factor loading represent the evolution of the factor space. A realized structural break can reveal the actual weight of idiosyncratic shocks, which may provide a clearer understanding of the true characteristics of granularity. While it is often natural to consider large actors as the most significant based on their size, size alone may

not fully capture the fundamental characteristics driving their systemic importance. We plan to explore these extensions in future research.

References

Acemoglu, D., Carvalho, V. M., Ozdaglar, A., & Tahbaz-Salehi, A. (2012). *The network origins of aggregate fluctuations* (Vol. 80; Tech. Rep. No. 5). Retrieved from https://onlinelibrary.wiley.com/doi/abs/10.3982/ECTA9623 doi: https://doi.org/10.3982/ECTA9623

Acemoglu, D., & Tahbaz-Salehi, A. (2020, July). *Firms, failures, and fluctuations: The macroeconomics of supply chain disruptions* (Working Paper No. 27565). National Bureau of Economic Research. Retrieved from http://www.nber.org/papers/w27565 doi: 10.3386/w27565

Bai, J., & Ng, S. (2002). Determining the number of factors in approximate factor models. *Econometrica*, *70*(1), 191-221. Retrieved from https://onlinelibrary.wiley.com/doi/abs/10.1111/1468-0262.00273 doi: https://doi.org/10.1111/1468-0262.00273

Ballester, C., Calvó-Armengol, A., & Zenou, Y. (2006). Who's who in networks. wanted: The key player. *Econometrica*, *74*(5), 1403–1417. Retrieved 2023-03-04, from http://www.jstor.org/stable/3805930

Baltagi, B. H., Kao, C., & Wang, F. (2021). Estimating and testing high dimensional factor models with multiple structural changes. *Journal of Econometrics*, *220*(2), 349-365. Retrieved from https://www.sciencedirect.com/science/article/pii/S030440762030124X (Annals Issue: Celebrating 40 Years of Panel Data Analysis: Past, Present and Future) doi: https://doi.org/10.1016/j.jeconom.2020.04.005

Banerjee, A., Marcellino, M., & Masten, I. (2008, 02). Chapter 4 forecasting macroeconomic variables using diffusion indexes in short samples with structural change. *Frontiers of Economics and Globalization*, *3*. doi: 10.1016/S1574-8715(07)00204-7

Baqaee, D. R. (2018). Cascading failures in production networks. *Econometrica*, *86*(5), 1819-1838. Retrieved from https://onlinelibrary.wiley.com/doi/abs/10.3982/ECTA15280 doi: https://doi.org/10.3982/ECTA15280

Barigozzi, M., & Brownlees, C. (2019). Nets:network estimation for time series. *Journal of Applied Econometrics*, *34*(3), 347-364. Retrieved from https://onlinelibrary.wiley.com/doi/abs/10.1002/jae.2676 doi: https://doi.org/10.1002/jae.2676

Barigozzi, M., Cho, H., & Fryzlewicz, P. (2018). Simultaneous multiple change-point and factor analysis for high-dimensional time series. *Journal of Econometrics*, *206*(1), 187-225. Retrieved from https://www.sciencedirect.com/science/article/pii/S0304407618300915 doi: https://doi.org/10.1016/j.jeconom.2018.05.003

Barigozzi, M., & Hallin, M. (2017). A network analysis of the volatility of high dimensional

financial series. *Journal of the Royal Statistical Society: Series C (Applied Statistics)*, *66*(3), 581-605. Retrieved from https://rss.onlinelibrary.wiley.com/doi/abs/10.1111/rssc.12177 doi: https://doi.org/10.1111/rssc.12177

Basu, S., & Rao, S. S. (2021). *Graphical models for nonstationary time series.* arXiv. Retrieved from https://arxiv.org/abs/2109.08709 doi: 10.48550/ARXIV.2109.08709

Basu, S., Shojaie, A., & Michailidis, G. (2015, jan). Network granger causality with inherent grouping structure. *J. Mach. Learn. Res.*, *16*(1), 417–453.

Bernanke, B. S., Boivin, J., & Eliasz, P. (2005, 02). Measuring the Effects of Monetary Policy: A Factor-Augmented Vector Autoregressive (FAVAR) Approach*. *The Quarterly Journal of Economics*, *120*(1), 387-422. Retrieved from https://doi.org/10.1162/0033553053327452 doi: 10.1162/0033553053327452

Bianchi, D., Billio, M., Casarin, R., & Guidolin, M. (2019). Modeling systemic risk with markov switching graphical sur models. *Journal of Econometrics*, *210*(1), 58-74. Retrieved from https://www.sciencedirect.com/science/article/pii/S0304407618302069 (Annals Issue in Honor of John Geweke "Complexity and Big Data in Economics and Finance: Recent Developments from a Bayesian Perspective") doi: https://doi.org/10.1016/j.jeconom.2018.11.005

Billio, M., Getmansky, M., Lo, A. W., & Pelizzon, L. (2012). Econometric measures of connectedness and systemic risk in the finance and insurance sectors. *Journal of Financial Economics*, *104*(3), 535-559. Retrieved from https://www.sciencedirect.com/science/article/pii/S0304405X11002868 (Market Institutions, Financial Market Risks and Financial Crisis) doi: https://doi.org/10.1016/j.jfineco.2011.12.010

Brownlees, C., Guðmundsson, G. S., & Lugosi, G. (2022). Community detection in partial correlation network models. *Journal of Business & Economic Statistics*, *40*(1), 216-226. Retrieved from https://doi.org/10.1080/07350015.2020.1798241 doi: 10.1080/07350015.2020.1798241

Brownlees, C., & Mesters, G. (2021). Detecting granular time series in large panels. *Journal of Econometrics*, *220*(2), 544-561. Retrieved from https://www.sciencedirect.com/science/article/pii/S0304407620301329 (Annals Issue: Celebrating 40 Years of Panel Data Analysis: Past, Present and Future) doi: https://doi.org/10.1016/j.jeconom.2020.04.013

Chamberlain, G., & Rothschild, M. (1983). Arbitrage, factor structure, and mean-variance analysis on large asset markets. *Econometrica*, *51*(5), 1281–1304. Retrieved 2023-12-17, from http://www.jstor.org/stable/1912275

Chen, L., Dolado, J. J., & Gonzalo, J. (2014). Detecting big structural breaks in large factor models. *Journal of Econometrics*, *180*(1), 30-48. Retrieved from https://www.sciencedirect.com/science/article/pii/S0304407614000189 doi: https://doi.org/10.1016/j.jeconom.2014.01.006

Chikuse, Y. (2003). *Statistics on special manifolds. lecture notes in statistics* (Vol. 174). doi: 10.1007/978-0-387-21540-2

Dahlhaus, R. (2000, Aug 01). Graphical interaction models for multivariate time series1. *Metrika*, *51*(2), 157-172. Retrieved from https://doi.org/10.1007/s001840000055 doi: 10.1007/s001840000055

Davis, C., & Kahan, W. M. (1970). The rotation of eigenvectors by a perturbation. iii. *SIAM Journal on Numerical Analysis*, *7*(1), 1–46. Retrieved 2022-09-01, from http://www.jstor.org/stable/2949580

Diebold, F. X., & Yılmaz, K. (2014). On the network topology of variance decompositions: Measuring the connectedness of financial firms. *Journal of Econometrics*, *182*(1), 119-134. Retrieved from https://www.sciencedirect.com/science/article/pii/S0304407614000712 (Causality, Prediction, and Specification Analysis: Recent Advances and Future Directions) doi: https://doi.org/10.1016/j.jeconom.2014.04.012

Edelman, A., Arias, T., & Smith, S. T. (1998). The geometry of algorithms with orthogonality constraints. *SIAM J. Matrix Anal. Appl.*, *20*, 303-353.

Eichler, M. (2012, Jun 01). Graphical modelling of multivariate time series. *Probability Theory and Related Fields*, *153*(1), 233-268. Retrieved from https://doi.org/10.1007/s00440-011-0345-8 doi: 10.1007/s00440-011-0345-8

Fan, J., Liao, Y., & Mincheva, M. (2013). Large covariance estimation by thresholding principal orthogonal complements. *Journal of the Royal Statistical Society. Series B (Statistical Methodology)*, *75*(4), 603–680. Retrieved 2022-08-31, from http://www.jstor.org/stable/24772450

Forni, M., Giannone, D., Lippi, M., & Reichlin, L. (2009). Opening the black box: Structural factor models with large cross sections. *Econometric Theory*, *25*(5), 1319–1347. Retrieved 2023-12-27, from http://www.jstor.org/stable/40388590

Gabaix, X. (2011). The granular origins of aggregate fluctuations. *Econometrica*, *79*(3), 733-772. Retrieved from https://onlinelibrary.wiley.com/doi/abs/10.3982/ECTA8769 doi: https://doi.org/10.3982/ECTA8769

Gabaix, X., & Koijen, R. S. J. (2021, June). *In search of the origins of financial fluctuations: The inelastic markets hypothesis* (Working Paper No. 28967). National Bureau of Economic Research. Retrieved from http://www.nber.org/papers/w28967

doi: 10.3386/w28967

Galeotti, A., Golub, B., & Goyal, S. (2020). Targeting interventions in networks. *Econometrica*, *88*(6), 2445-2471. Retrieved from https://onlinelibrary.wiley.com/doi/abs/10.3982/ECTA16173 doi: https://doi.org/10.3982/ECTA16173

Gaubert, C., & Itskhoki, O. (2021). Granular Comparative Advantage. *Journal of Political Economy*, *129*(3), 871-939. Retrieved from https://ideas.repec.org/a/ucp/jpolec/doi10.1086-712444.html doi: 10.1086/712444

Guðmundsson, G. S., & Brownlees, C. (2021). Detecting groups in large vector autoregressions. *Journal of Econometrics*, *225*(1), 2-26. Retrieved from https://www.sciencedirect.com/science/article/pii/S030440762100124X (Themed Issue: Vector Autoregressions) doi: https://doi.org/10.1016/j.jeconom.2021.03.012

Heipertz, J., Ouazad, A., & Rancière, R. (2019, July). *The transmission of shocks in endogenous financial networks: A structural approach* (Working Paper No. 26049). National Bureau of Economic Research. Retrieved from http://www.nber.org/papers/w26049 doi: 10.3386/w26049

Horn, R. A., & Johnson, C. R. (2013). *Matrix analysis* (2nd ed.). Cambridge; New York: Cambridge University Press.

Ma, S., & Su, L. (2018). Estimation of large dimensional factor models with an unknown number of breaks. *Journal of Econometrics*, *207*(1), 1-29. Retrieved from https://www.sciencedirect.com/science/article/pii/S0304407618301155 doi: https://doi.org/10.1016/j.jeconom.2018.06.019

Massacci, D. (2021, 10). Testing for Regime Changes in Portfolios with a Large Number of Assets: A Robust Approach to Factor Heteroskedasticity*. *Journal of Financial Econometrics*, *21*(2), 316-367. Retrieved from https://doi.org/10.1093/jjfinec/nbaa046 doi: 10.1093/jjfinec/nbaa046

Mazzarisi, P., Lillo, F., & Marmi, S. (2019). When panic makes you blind: A chaotic route to systemic risk. *Journal of Economic Dynamics and Control*, *100*, 176-199. Retrieved from https://www.sciencedirect.com/science/article/pii/S0165188919300053 doi: https://doi.org/10.1016/j.jedc.2018.12.009

Merlevède, F., Peligrad, M., & Rio, E. (2011, Dec 01). A bernstein type inequality and moderate deviations for weakly dependent sequences. *Probability Theory and Related Fields*, *151*(3), 435-474. Retrieved from https://doi.org/10.1007/s00440-010-0304-9 doi: 10.1007/s00440-010-0304-9

Parker, J., & Sul, D. (2016). Identification of unknown common factors: Leaders and followers. *Journal of Business & Economic Statistics*, *34*(2), 227-239. Retrieved from https://doi.org/10.1080/07350015.2015.1026439 doi: 10.1080/07350015

.2015.1026439

Pourahmadi, M. (2013). High-dimensional covariance estimation. *Copyright © 2013 John Wiley Sons, Inc. All rights reserved*, *Wiley Series in Probability and Statistics*. doi: DOI:10.1002/9781118573617

Ross, S. A. (1976). The arbitrage theory of capital asset pricing. *Journal of Economic Theory*, *13*(3), 341-360. Retrieved from https://www.sciencedirect.com/science/article/pii/0022053176900466 doi: https://doi.org/10.1016/0022-0531(76)90046-6

Stock, J. H., & Watson, M. W. (2002a). Forecasting using principal components from a large number of predictors. *Journal of the American Statistical Association*, *97*(460), 1167–1179. Retrieved 2023-02-14, from http://www.jstor.org/stable/3085839

Stock, J. H., & Watson, M. W. (2002b). Macroeconomic forecasting using diffusion indexes. *Journal of Business & Economic Statistics*, *20*(2), 147-162. Retrieved from https://doi.org/10.1198/073500102317351921 doi: 10.1198/073500102317351921

Stock, J. H., & Watson, M. W. (2009, 04). 1737 Forecasting in Dynamic Factor Models Subject to Structural Instability. In *The Methodology and Practice of Econometrics: A Festschrift in Honour of David F. Hendry.* Oxford University Press. Retrieved from https://doi.org/10.1093/acprof:oso/9780199237197.003.0007 doi: 10.1093/acprof:oso/9780199237197.003.0007

Tao, T. (2023). *Topics in random matrix theory.* American Mathematical Soc. Retrieved from https://books.google.de/books?id=Hjq_JHLNPT0C

Taschereau-Dumouchel, M. (2019, 01). Cascades and fluctuations in an economy with an endogenous production network. *SSRN Electronic Journal*. doi: 10.2139/ssrn.3115854

Wang, W., & Fan, J. (2017). Asymptotics of empirical eigenstructure for high dimensional spiked covariance. *The Annals of Statistics*, *45*(3), 1342–1374. Retrieved 2023-06-18, from http://www.jstor.org/stable/26362833

Yamamoto, Y. (2016). Forecasting with nonspurious factors in u.s. macroeconomic time series. *Journal of Business Economic Statistics*, *34*(1), 81–106. Retrieved 2023-12-18, from http://www.jstor.org/stable/44164735

Yu, Y., Wang, T., & Samworth, R. J. (2015). A useful variant of the davis—kahan theorem for statisticians. *Biometrika*, *102*(2), 315–323. Retrieved 2022-09-01, from http://www.jstor.org/stable/43908537

A Proofs

Additional Notations $a \wedge b \equiv \min(a,b)$ and $a \vee b \equiv \max(a,b)$. $a \lesssim b$ if $a \leq cb$ for some constant $c > 0$. For a simple exposition, *let us omit **all** the subscript '0' for the present regime.*

Section 3

PROPOSITION 1. Under the model assumptions, for large N,

$$d\Big(\text{span}(P_0), \text{span}(P_1)\Big) = \text{tr}\Big(\Sigma_{u,0}\Sigma_{y,0}^{-1}P_1P_1'\Sigma_{y,0}^{-1}\Sigma_{u,0}\Big) + o(1). \tag{11}$$

Proof.

$$d\Big(\text{span}(P), \text{span}(P_1)\Big) = \text{tr}\Big(P_\perp P_\perp' P_1 P_1' P_\perp P_\perp'\Big) = \text{tr}\Big(P_\perp P_\perp' \Sigma_y \Sigma_y^{-1} P_1 P_1' \Sigma_y^{-1} \Sigma_y P_\perp P_\perp'\Big)$$

As $\Sigma_y = \Sigma_\chi + \Sigma_u$ where the low dimensional component has orthogonal decomposition $\Sigma_\chi = P\Sigma_f P'$,

$$\begin{aligned}\text{tr}\Big(P_\perp P_\perp' \Sigma_y \Sigma_y^{-1} P_1 P_1' \Sigma_y^{-1} \Sigma_y P_\perp P_\perp'\Big) &= \text{tr}\Big(P_\perp P_\perp' \Sigma_u \Sigma_y^{-1} P_1 P_1' \Sigma_y^{-1} \Sigma_u P_\perp P_\perp'\Big) \\ &= \text{tr}\Big(\Sigma_u \Sigma_y^{-1} P_1 P_1' \Sigma_y^{-1} \Sigma_u P_\perp P_\perp'\Big)\end{aligned}$$

by the cyclic invariance of the trace. As $P_\perp P_\perp' = I_N - PP'$,

$$d\Big(\text{span}(P), \text{span}(P_1)\Big) = \text{tr}\Big(\Sigma_u \Sigma_y^{-1} P_1 P_1' \Sigma_y^{-1} \Sigma_u\Big) - \text{tr}\Big(\Sigma_u \Sigma_y^{-1} P_1 P_1' \Sigma_y^{-1} \Sigma_u PP'\Big). \tag{31}$$

The last term of (31) equals $\text{tr}\Big(P_1'\Sigma_y^{-1}\Sigma_u PP'\Sigma_u\Sigma_y^{-1}P_1\Big) = \text{tr}\Big[\Sigma_y^{-1}\Sigma_u PP'\Sigma_u\Sigma_y^{-1}\,|\,\text{span}(P_1)\Big]$, the partial trace confining the domain of the quadratic operation of $\Sigma_y^{-1}\Sigma_u PP'\Sigma_u\Sigma_y^{-1}$ to $v \in \text{span}(P_1)$. That is, it is defined for any orthonormal basis $\{\mathbf{v}_k\}_{k=1,\dots,K_1}$ of $\text{span}(P_1)$,

$$\text{tr}\Big[\Sigma_y^{-1}\Sigma_u PP'\Sigma_u\Sigma_y^{-1}\,|\,\text{span}(P_1)\Big] \equiv \sum_{k=1}^{K_1} \mathbf{v}_k'\Sigma_y^{-1}\Sigma_u PP'\Sigma_u\Sigma_y^{-1}\mathbf{v}_k.$$

It is bounded by the whole trace, as $\text{tr}\Big(\Sigma_y^{-1}\Sigma_u PP'\Sigma_u\Sigma_y^{-1}\Big) \geq \sum_{\kappa=1}^{K_1}\lambda_\kappa$ for the eigenvalues $\{\lambda_\kappa\}$ of $\Sigma_y^{-1}\Sigma_u PP'\Sigma_u\Sigma_y^{-1}$ in descending order[17], and the summation of the first K_1 eigenvalues are the supremum of the partial trace confined to all possible subspaces V of dimension K_1 in the entire N dimension (Tao (2023) Proposition 1.3.4): $\sum_{\kappa=1}^{K_1}\lambda_\kappa = \sup_{V,\,\dim(V)=K_1}\text{tr}[\Sigma_y^{-1}\Sigma_u PP'\Sigma_u\Sigma_y^{-1}|V]$.

[17] $\lambda_\kappa \geq 0, \forall \kappa = 1,\dots,N$ as the eigenvalues of a product of positive semidefinite matrices.

Now we focus on $\mathrm{tr}[\Sigma_y^{-1}\Sigma_u PP'\Sigma_u\Sigma_y^{-1}]$. Let $\tilde{P}$ be a column-augmented orthonormal basis of the principle subspace corresponding to the K largest eigenvalues of Σ_y. As the eigenvectors are invariant under the matrix inversion, Σ_y^{-1} has the orthogonal spectral decomposition with respect to $\tilde{P}$, such that $\Sigma_y^{-1} = \tilde{P}\tilde{P}'\Sigma_y^{-1}\tilde{P}\tilde{P}' + \tilde{P}_\perp\tilde{P}_\perp'\Sigma_y^{-1}\tilde{P}_\perp\tilde{P}_\perp' (= \tilde{P}\tilde{\Lambda}_1\tilde{P}' + \tilde{P}_\perp\tilde{\Lambda}_2\tilde{P}_\perp')$. Accordingly, $\mathrm{tr}[\Sigma_y^{-1}\Sigma_u PP'\Sigma_u\Sigma_y^{-1}]\big(=: \boxed{1}\big)$ can be decomposed as follows:

$$
\begin{aligned}
\boxed{1} = {} & \mathrm{tr}[\Sigma_y^{-1}\tilde{P}\tilde{P}'\Sigma_u\tilde{P}\tilde{P}'PP'\tilde{P}\tilde{P}'\Sigma_u\tilde{P}\tilde{P}'\Sigma_y^{-1}] + 2\mathrm{tr}[\Sigma_y^{-1}\tilde{P}\tilde{P}'\Sigma_u\tilde{P}_\perp\tilde{P}_\perp'PP'\tilde{P}\tilde{P}'\Sigma_u\tilde{P}\tilde{P}'\Sigma_y^{-1}] \\
& + 2\mathrm{tr}[\Sigma_y^{-1}\tilde{P}_\perp\tilde{P}_\perp'\Sigma_u\tilde{P}_\perp\tilde{P}_\perp'PP'\tilde{P}\tilde{P}'\Sigma_u\tilde{P}_\perp\tilde{P}_\perp'\Sigma_y^{-1}] + \mathrm{tr}[\Sigma_y^{-1}\tilde{P}\tilde{P}'\Sigma_u\tilde{P}_\perp\tilde{P}_\perp'PP'\tilde{P}_\perp\tilde{P}_\perp'\Sigma_u\tilde{P}\tilde{P}'\Sigma_y^{-1}] \\
& + \mathrm{tr}[\Sigma_y^{-1}\tilde{P}_\perp\tilde{P}_\perp'\Sigma_u\tilde{P}_\perp\tilde{P}_\perp'PP'\tilde{P}_\perp\tilde{P}_\perp'\Sigma_u\tilde{P}_\perp\tilde{P}_\perp'\Sigma_y^{-1}] + \mathrm{tr}[\Sigma_y^{-1}\tilde{P}_\perp\tilde{P}_\perp'\Sigma_u\tilde{P}\tilde{P}'PP'\tilde{P}\tilde{P}'\Sigma_u\tilde{P}_\perp\tilde{P}_\perp'\Sigma_y^{-1}],
\end{aligned}
$$

since any terms involving $\tilde{P}\tilde{P}'\Sigma_y^{-2}\tilde{P}_\perp\tilde{P}_\perp'$ after a cyclic transformation of the argument of the trace operation vanish as Σ_y^{-2} shares the same basis of the spectral decomposition as Σ_y^{-1}.

Let us number the six terms of $\boxed{1}$ as $\boxed{1}$ **-1** to $\boxed{1}$ **-6**. The following properties will be repeatedly employed to give a bound on each term, mainly jointly applied with the matrix Cauchy-Schwarz inequality (stated below) on products of positive semidefinite matrices and the trace cyclicity.

Properties 1.

(a) $\mathrm{tr}[\tilde{P}'\Sigma_u^2\tilde{P}] \le K\|\Sigma_u^2\| = O(1)$, by Assumption 2.

(b) $\mathrm{tr}[\tilde{P}\tilde{P}'\Sigma_y^{-2}\tilde{P}\tilde{P}'] \le K\|\tilde{\Lambda}_1^2\| = o(1)$, by Assumption 1.

(c) $\|\tilde{P}_\perp\tilde{P}_\perp'PP'\|_F^2 = O(N^{-2})$ by **The sin$\boldsymbol{\theta}$ Theorem** (Davis and Kahan (1970)) with Assumption 1 and 2.

(d) $\|\tilde{P}_\perp\tilde{P}_\perp'\Sigma_u\tilde{P}\tilde{P}'\|_F^2 = O(N^{-2})$, by Assumption 1-3, and the above property (c).

Matrix Cauchy-Schwarz Inequality Let * denote the Hermitian operator (the transpose of the complex conjugation). For any complex (or real) matrices A,B of the same sizes, the trace operation $\mathrm{tr}(B^*A)(= \mathrm{tr}(A^*B))$ defines an inner product (the *Frobenius inner product*, Horn and Johnson (2013)(5.2.7))

$$
\langle A, B\rangle_F \equiv \mathrm{tr}(B^*A)(= \mathrm{tr}(B'A) \text{ for real matrices}).
$$

Hence, it equips an inner product on the space of complex (or real) matrices of the same sizes. The Cauchy-Schwarz inequality $\langle A, B\rangle_F^2 \le \langle A, A\rangle_F\langle B, B\rangle_F$ is naturally inherited

on this inner product space. That is, for the case of the space of real matrices of the same sizes,

$$|\mathrm{tr}(A'B)| \le [\mathrm{tr}(A'A)]^{1/2}[\mathrm{tr}(B'B)]^{1/2} (= \|A\|_F \|B\|_F). \tag{32}$$

(it implies that the trace is submultiplicative on positive semidefinite matrices.)

A term-by-term inspection of $\boxed{1}$ follows.

$\boxed{1}$ **-1:** $\mathrm{tr}[\Sigma_y^{-1}\tilde{P}\tilde{P}'\Sigma_u\tilde{P}\tilde{P}'PP'\tilde{P}\tilde{P}'\Sigma_u\tilde{P}\tilde{P}'\Sigma_y^{-1}] = \mathrm{tr}[\Sigma_u\tilde{P}\tilde{P}'PP'\tilde{P}\tilde{P}'\Sigma_u\tilde{P}\tilde{P}'\Sigma_y^{-2}\tilde{P}\tilde{P}']$ due to the cyclicity. As the trace is submultiplicative on positive semidefinite matrices, it is bounded as

$$\mathrm{tr}[\Sigma_u\tilde{P}\tilde{P}'PP'\tilde{P}\tilde{P}'\Sigma_u\tilde{P}\tilde{P}'\Sigma_y^{-2}\tilde{P}\tilde{P}'] \le \mathrm{tr}[\Sigma_u\tilde{P}\tilde{P}'PP'\tilde{P}\tilde{P}'\Sigma_u]\mathrm{tr}[\tilde{P}\tilde{P}'\Sigma_y^{-2}\tilde{P}\tilde{P}'] = o(1),$$

since $\mathrm{tr}[\Sigma_u\tilde{P}\tilde{P}'PP'\tilde{P}\tilde{P}'\Sigma_u] = \mathrm{tr}[\tilde{P}'\Sigma_u^2\tilde{P}\,|\,\mathrm{span}(P)] \le \mathrm{tr}[\tilde{P}'\Sigma_u^2\tilde{P}] = O(1)$ by (a), and $\mathrm{tr}[\tilde{P}\tilde{P}'\Sigma_y^{-2}\tilde{P}\tilde{P}'] = o(1)$ by (b).

$\boxed{1}$ **-2:** $\mathrm{tr}[\Sigma_y^{-1}\tilde{P}\tilde{P}'\Sigma_u\tilde{P}_\perp\tilde{P}_\perp'PP'\tilde{P}\tilde{P}'\Sigma_u\tilde{P}\tilde{P}'\Sigma_y^{-1}] = \mathrm{tr}[\Sigma_u\tilde{P}_\perp\tilde{P}_\perp'PP'\tilde{P}\tilde{P}'\Sigma_u\tilde{P}\tilde{P}'\Sigma_y^{-2}\tilde{P}\tilde{P}']$ due to the cyclicity. Let us denote $A \coloneqq \Sigma_u\tilde{P}_\perp\tilde{P}_\perp'PP'\tilde{P}\tilde{P}'\Sigma_u$. By the Cauchy-Schwarz (32),

$$\mathrm{tr}[\Sigma_u\tilde{P}_\perp\tilde{P}_\perp'PP'\tilde{P}\tilde{P}'\Sigma_u\tilde{P}\tilde{P}'\Sigma_y^{-2}\tilde{P}\tilde{P}'] \le [\mathrm{tr}(A'A)]^{1/2}\mathrm{tr}(\tilde{P}\tilde{P}'\Sigma_y^{-2}\tilde{P}\tilde{P}'). \tag{33}$$

Let us observe that, by the cyclicity and the submultiplicativity of the trace,

$$\begin{aligned}\mathrm{tr}(A'A) &= \mathrm{tr}(\Sigma_u\tilde{P}\tilde{P}'PP'\tilde{P}_\perp\tilde{P}_\perp'\Sigma_u^2\tilde{P}_\perp\tilde{P}_\perp'PP'\tilde{P}\tilde{P}'\Sigma_u)\\ &\le \mathrm{tr}[PP'\tilde{P}_\perp\tilde{P}_\perp'\Sigma_u^2\tilde{P}_\perp\tilde{P}_\perp'PP']\mathrm{tr}(\tilde{P}\tilde{P}'\Sigma_u^2\tilde{P}\tilde{P}').\end{aligned} \tag{34}$$

The last component $\mathrm{tr}(\tilde{P}\tilde{P}'\Sigma_u^2\tilde{P}\tilde{P}') = O(1)$ by (a). The other part,

$$\mathrm{tr}[PP'\tilde{P}_\perp\tilde{P}_\perp'\Sigma_u^2\tilde{P}_\perp\tilde{P}_\perp'PP'] \le \|PP'\tilde{P}_\perp\tilde{P}_\perp'\|_F^2\mathrm{tr}(\Sigma_u^2) = O(N^{-1}) = o(1), \tag{35}$$

since $\|PP'\tilde{P}_\perp\tilde{P}_\perp'\|_F^2 = O(N^{-2})$ by (c) and $\mathrm{tr}(\Sigma_u^2) \le N\|\Sigma_u^2\| = O(N)$ by Assumption 2. Hence $\mathrm{tr}(A'A) = o(1)$ in (34). As the last component in (33), $\mathrm{tr}(\tilde{P}\tilde{P}'\Sigma_y^{-2}\tilde{P}\tilde{P}') = o(1)$ by (b), $\boxed{1}$ -2 (up to the factor 2) is bounded by $o(1)$.

$\boxed{1}$ **-3:** By the cyclicity, the orthonormality $\tilde{P}_\perp'\tilde{P}_\perp = I_{N-K}$, and (32), $\boxed{1}$ -3 is bounded (up to the factor 2) such as

$$\mathrm{tr}[\Sigma_y^{-1}\tilde{P}_\perp\tilde{P}_\perp'\Sigma_u\tilde{P}_\perp\tilde{P}_\perp'PP'\tilde{P}\tilde{P}'\Sigma_u\tilde{P}_\perp\tilde{P}_\perp'\tilde{P}_\perp\tilde{P}_\perp'\Sigma_y^{-1}] \le [\mathrm{tr}(B'B)]^{1/2}\mathrm{tr}(\tilde{P}_\perp\tilde{P}_\perp'\Sigma_y^{-2}\tilde{P}_\perp\tilde{P}_\perp'), \tag{36}$$

where $B := \Sigma_u \tilde{P}_\perp \tilde{P}_\perp' PP' \tilde{P}\tilde{P}' \Sigma_u \tilde{P}_\perp \tilde{P}_\perp'$. Then due to (35) above and (d),

$$\begin{aligned}\mathrm{tr}(B'B) &= \mathrm{tr}[\tilde{P}_\perp \tilde{P}_\perp' \Sigma_u \tilde{P}\tilde{P}' PP' \tilde{P}_\perp \tilde{P}_\perp' \Sigma_u^2 \tilde{P}_\perp \tilde{P}_\perp' PP' \tilde{P}\tilde{P}' \Sigma_u \tilde{P}_\perp \tilde{P}_\perp'] \\ &\le \mathrm{tr}[PP' \tilde{P}_\perp \tilde{P}_\perp' \Sigma_u^2 \tilde{P}_\perp \tilde{P}_\perp' PP'] \|\tilde{P}\tilde{P}' \Sigma_u \tilde{P}_\perp \tilde{P}_\perp'\|_F^2 = O(N^{-3}).\end{aligned}$$

Alongside with $\mathrm{tr}(\tilde{P}_\perp \tilde{P}_\perp' \Sigma_y^{-2} \tilde{P}_\perp \tilde{P}_\perp') \le (N-K)\|\Sigma_y^{-2}\| = O(N-K)$, (36) gives an $o(1)$ bound.

$\boxed{1}$ **-4:** $\mathrm{tr}[\Sigma_y^{-1} \tilde{P}\tilde{P}' \Sigma_u \tilde{P}_\perp \tilde{P}_\perp' PP' \tilde{P}_\perp \tilde{P}_\perp' \Sigma_u \tilde{P}\tilde{P}' \Sigma_y^{-1}] = \mathrm{tr}[\Sigma_u \tilde{P}_\perp \tilde{P}_\perp' PP' \tilde{P}_\perp \tilde{P}_\perp' \Sigma_u \tilde{P}\tilde{P}' \Sigma_y^{-2} \tilde{P}\tilde{P}'] \le \mathrm{tr}[\Sigma_u \tilde{P}_\perp \tilde{P}_\perp' PP' \tilde{P}_\perp \tilde{P}_\perp' \Sigma_u] \mathrm{tr}[\tilde{P}\tilde{P}' \Sigma_y^{-2} \tilde{P}\tilde{P}'] = \mathrm{tr}[PP' \tilde{P}_\perp \tilde{P}_\perp' \Sigma_u^2 \tilde{P}_\perp \tilde{P}_\perp' PP'] \mathrm{tr}[\tilde{P}\tilde{P}' \Sigma_y^{-2} \tilde{P}\tilde{P}'] = o(1)$, by the trace cyclicity and the submultiplicativity, (35), and (b).

$\boxed{1}$ **-5:** By the trace cyclicity and the submultiplicativity and (c),

$$\begin{aligned}&\mathrm{tr}[\Sigma_y^{-1} \tilde{P}_\perp \tilde{P}_\perp' \Sigma_u \tilde{P}_\perp \tilde{P}_\perp' PP' \tilde{P}_\perp \tilde{P}_\perp' \Sigma_u \tilde{P}_\perp \tilde{P}_\perp' \Sigma_y^{-1}] \\ &\le \mathrm{tr}[\tilde{P}_\perp \tilde{P}_\perp' PP' \tilde{P}_\perp \tilde{P}_\perp'] \mathrm{tr}[\Sigma_u \tilde{P}_\perp \tilde{P}_\perp' \Sigma_y^{-2} \tilde{P}_\perp \tilde{P}_\perp' \Sigma_u] = O(N^{-2}) \mathrm{tr}[\Sigma_u \tilde{P}_\perp \tilde{P}_\perp' \Sigma_y^{-2} \tilde{P}_\perp \tilde{P}_\perp' \Sigma_u] \qquad (37)\end{aligned}$$

Again by the cyclicity, $\mathrm{tr}[\Sigma_u \tilde{P}_\perp \tilde{P}_\perp' \Sigma_y^{-2} \tilde{P}_\perp \tilde{P}_\perp' \Sigma_u] = \mathrm{tr}[\tilde{P}_\perp' \Sigma_y^{-2} \tilde{P}_\perp \tilde{P}_\perp' \Sigma_u^2 \tilde{P}_\perp]$
$\le \mathrm{tr}[\Sigma_y^{-2} \tilde{P}_\perp \tilde{P}_\perp' \Sigma_u^2 | \mathrm{span}(\tilde{P}_\perp)] \le \mathrm{tr}[\Sigma_y^{-2} \tilde{P}_\perp \tilde{P}_\perp' \Sigma_u^2] \le (N-K)\|\Sigma_u^2 \Sigma_y^{-2}\| = O(N-K)$,which completes an o(1) bound in (37)

$\boxed{1}$ **-6:** Due to the cyclicity, the submultiplicativity, and (d),

$$\begin{aligned}&\mathrm{tr}[\Sigma_y^{-1} \tilde{P}_\perp \tilde{P}_\perp' \Sigma_u \tilde{P}\tilde{P}' PP' \tilde{P}\tilde{P}' \Sigma_u \tilde{P}_\perp \tilde{P}_\perp' \Sigma_y^{-1}] \le \mathrm{tr}[\tilde{P}_\perp \tilde{P}_\perp' \Sigma_u \tilde{P}\tilde{P}' PP' \tilde{P}\tilde{P}' \Sigma_u \tilde{P}_\perp \tilde{P}_\perp'] \mathrm{tr}[\Sigma_y^{-2}] \\ &= \mathrm{tr}\big[\tilde{P}\tilde{P}' \Sigma_u \tilde{P}_\perp \tilde{P}_\perp' \Sigma_u \tilde{P}\tilde{P}' | \mathrm{span}(P)\big] O(N) \le \|\tilde{P}\tilde{P}' \Sigma_u \tilde{P}_\perp \tilde{P}_\perp'\|_F^2 O(N) = O(N^{-2}) O(N) = o(1).\end{aligned}$$

Therefore, $\boxed{1} := \mathrm{tr}[\Sigma_y^{-1} \Sigma_u PP' \Sigma_u \Sigma_y^{-1}] = o(1)$ and

$$d\big(\mathrm{span}(P), \mathrm{span}(P_1)\big) = \mathrm{tr}\Big(\Sigma_u \Sigma_y^{-1} P_1 P_1' \Sigma_y^{-1} \Sigma_u\Big) + o(1) \qquad (11)$$

□

Section 4.1

Standard procedures of Factor Loading Estimation

Let

$$Y = BF + U \qquad (17)$$

under Assumptions 1-2, 6-10 in the 2.1.1 and 4.1. The discussion is for any given, fixed regime, omitting the regime index j. Standard[18] procedures of estimating factor loading are as follows: First, B can be estimated by $\hat{B} = \sqrt{N}\hat{P}_N$, where $\hat{P}_N$ is the column

[18]Following in many classical studies such as Bai and Ng (2002), Stock and Watson (2002a).

augmentation of $K-$ dominant orthonormal eigenvectors of the sample covariance matrix $(1/T)YY'$. Second, it can be estimated by $\tilde{B} = (1/\sqrt{T})Y\hat{P}_T$, for $\hat{P}_T$ the column augmentation of $K-$ dominant eigenvectors of $(1/N)Y'Y$.
The columns of $\tilde{B}$ span the same space as the $K-$ dominant eigenvectors of $(1/T)YY'$: There exists diagonal matrix Σ_N^K of the $K-$ largest eigenvalues of $(1/N)Y'Y$ such that the rank K linear combination $\tilde{B}((N/T)\Sigma_N^K)^{-1/2}$ of the columns of $\tilde{B}$ gives

$$\begin{aligned}&((N/T)\Sigma_N^K)^{-1/2}\tilde{B}'(1/T)YY'\tilde{B}((N/T)\Sigma_N^K)^{-1/2}\\&= (N/T)(\Sigma_N^K)^{-1/2}\hat{P}_T'(1/N)(Y'Y)(1/N)(Y'Y)\hat{P}_T(\Sigma_N^K)^{-1/2} = (N/T)\Sigma_N^K = \Sigma_T^K\end{aligned}$$

which is the diagonal matrix of $K-$ largest eigenvalues of $(1/T)YY'$. Hence, the resulting (factor) spaces spanned by $\hat{B}$ (or $\hat{P}_N$) and $\tilde{B}$ are identical.

The K_j- Principal Subspace Consistency The leading K_j- principal subspace $\text{span}(\hat{P}_j)$ of $\hat{\Sigma}_{y,j}^{\text{sam}}$ or $\hat{\Sigma}_{\chi,j} = \hat{\Sigma}_{y,j}^{K_j}$, the spectral decomposition of $\hat{\Sigma}_{y,j}^{\text{sam}}$ up to K_j, deviates from $\text{span}(P_j)$ by $o_p(1)$, by Yu, Wang, and Samworth (2015): Measured by the projector metric $d(\text{span}(\hat{P}_j), \text{span}(P_j)) \equiv \|\mathcal{P}_j^{\perp}\hat{\mathcal{P}}_j\|_F$,

$$\|\mathcal{P}_j^{\perp}\hat{\mathcal{P}}_j\|_F \lesssim \|\hat{\Sigma}_{\chi,j} - \Sigma_{\chi,j}\|/\lambda_{\chi,j}^{K_j} \leq \left(\|\hat{\Sigma}_{\chi,j} - \Sigma_{y,j}^{K_j}\| + \|\Sigma_{u,j}\|\right)/\lambda_{\chi,j}^{K_j} = o_p(1), \tag{38}$$

for $\Sigma_{y,j}^{K_j}$ the spectral decomposition of $\Sigma_{y,j}$ up to K_j. The numerator comes by the triangle inequality $\|\hat{\Sigma}_{\chi,j} - \Sigma_{\chi,j}\| \leq \|\hat{\Sigma}_{\chi,j} - \Sigma_{y,j}^{K_j}\| + \|\Sigma_{y,j}^{K_j} - \Sigma_{\chi,j}\|$. The latter is bounded by $\|\Sigma_{u,j}\|$, the source of the population level deviation. The denominator $|\hat{\lambda}_{\chi,j}^{K_j+1} - \lambda_{\chi,j}^{K_j}| = \lambda_{\chi,j}^{K_j}$ as $\hat{\Sigma}_{\chi,j}$ has the same rank as $\Sigma_{\chi,j}$. As $\|\hat{\Sigma}_{\chi,j} - \Sigma_{y,j}^{K_j}\| \lesssim \|\hat{\Sigma}_{y,j}^{\text{sam}} - \Sigma_{y,j}\| = o_p(N)$ (due to Lemma 4 of Fan et al. (2013)) and $\lambda_{\chi,j}^{K_j} = O(N)$, $d(\text{span}(\hat{P}_j), \text{span}(P_j)) = o_p(1)$.

Proposition 2. Under the Assumptions 1-2 in 2.1.1 and 6-11 in 4.1, the event

$$\Upsilon \equiv \left\{\|\hat{\mathcal{I}}_g\| > \|\hat{\mathcal{I}}_i\| \,|\, g \in \mathcal{G}, i \in \mathcal{G}^c\right\} \tag{24}$$

holds asymptotically almost surely.

Proof. We first prove the following claim for any matrix norm $\|\cdot\|$:

Claim: $\|\hat{\mathcal{I}} - \mathcal{I}\| = o_p(1)$ for $\mathcal{I} \equiv \|\Sigma_y^{-1}P_1P_1'\Sigma_y^{-1}\Sigma_u\|$ and $\hat{\mathcal{I}}_i = \left\|\hat{\Sigma}_y^{-1}\hat{P}_1\hat{P}_1'\hat{\Sigma}_y^{-1}\hat{\Sigma}_u\right\|$ following the estimation procedure in Section 4.1 for $\omega_{T,j} = o(1)$.

Proof of the Claim: Observe that, by simply adding and subtracting terms,

$$\begin{aligned}\hat{\mathcal{I}} - \mathcal{I} = &(\hat{\Sigma}_y^{-1} - \Sigma_y^{-1})(\hat{P}_1\hat{P}_1' - P_1P_1')\hat{\Sigma}_y^{-1}(\hat{\Sigma}_u - \Sigma_u) + (\hat{\Sigma}_y^{-1} - \Sigma_y^{-1})(\hat{P}_1\hat{P}_1' - P_1P_1')\hat{\Sigma}_y^{-1}\Sigma_u \\ &+ (\hat{\Sigma}_y^{-1} - \Sigma_y^{-1})P_1P_1'\hat{\Sigma}_y^{-1}(\hat{\Sigma}_u - \Sigma_u) + (\hat{\Sigma}_y^{-1} - \Sigma_y^{-1})P_1P_1'\hat{\Sigma}_y^{-1}\Sigma_u \\ &+ \Sigma_y^{-1}(\hat{P}_1\hat{P}_1' - P_1P_1')\hat{\Sigma}_y^{-1}(\hat{\Sigma}_u - \Sigma_u) + \Sigma_y^{-1}(\hat{P}_1\hat{P}_1' - P_1P_1')\hat{\Sigma}_y^{-1}\Sigma_u \\ &+ \Sigma_y^{-1}P_1P_1'\hat{\Sigma}_y^{-1}(\hat{\Sigma}_u - \Sigma_u) + \Sigma_y^{-1}P_1P_1'(\hat{\Sigma}_y^{-1} - \Sigma_y^{-1})\Sigma_u.\end{aligned}$$

By the triangle inequality,

$$\begin{aligned}\|\hat{\mathcal{I}} - \mathcal{I}\| \le &\|\hat{\Sigma}_y^{-1} - \Sigma_y^{-1}\|\|\hat{P}_1\hat{P}_1' - P_1P_1'\|\|\Sigma_y^{-1}\|\|\hat{\Sigma}_u - \Sigma_u\| \\ &+ \|\hat{\Sigma}_y^{-1} - \Sigma_y^{-1}\|\|\hat{P}_1\hat{P}_1' - P_1P_1'\|o_p(1)\|\hat{\Sigma}_u - \Sigma_u\| \\ &+ \|\hat{\Sigma}_y^{-1} - \Sigma_y^{-1}\|\|\hat{P}_1\hat{P}_1' - P_1P_1'\|\|\Sigma_y^{-1}\|\|\Sigma_u\| + \|\hat{\Sigma}_y^{-1} - \Sigma_y^{-1}\|\|\hat{P}_1\hat{P}_1' - P_1P_1'\|o_p(1)\|\Sigma_u\| \\ &+ \|\hat{\Sigma}_y^{-1} - \Sigma_y^{-1}\|\|P_1P_1'\|\|\Sigma_y^{-1}\|\|\hat{\Sigma}_u - \Sigma_u\| + \|\hat{\Sigma}_y^{-1} - \Sigma_y^{-1}\|\|P_1P_1'\|o_p(1)\|\hat{\Sigma}_u - \Sigma_u\| \\ &+ \|\hat{\Sigma}_y^{-1} - \Sigma_y^{-1}\|\|P_1P_1'\|\|\Sigma_y^{-1}\|\|\Sigma_u\| + \|\hat{\Sigma}_y^{-1} - \Sigma_y^{-1}\|\|P_1P_1'\|o_p(1)\|\Sigma_u\| \\ &+ \|\Sigma_y^{-1}\|^2\|\hat{P}_1\hat{P}_1' - P_1P_1'\|\|\hat{\Sigma}_u - \Sigma_u\| + \|\Sigma_y^{-1}\|\|\hat{P}_1\hat{P}_1' - P_1P_1'\|o_p(1)\|\hat{\Sigma}_u - \Sigma_u\| \\ &+ \|\Sigma_y^{-1}\|^2\|\hat{P}_1\hat{P}_1' - P_1P_1'\|\|\Sigma_u\| + \|\Sigma_y^{-1}\|\|\hat{P}_1\hat{P}_1' - P_1P_1'\|o_p(1)\|\Sigma_u\| \\ &+ \|\Sigma_y^{-1}\|^2\|P_1P_1'\|\|\hat{\Sigma}_u - \Sigma_u\| + \|\Sigma_y^{-1}\|\|P_1P_1'\|o_p(1)\|\hat{\Sigma}_u - \Sigma_u\| \\ &+ \|\Sigma_y^{-1}\|\|P_1P_1'\|\|\hat{\Sigma}_y^{-1} - \Sigma_y^{-1}\|\|\Sigma_u\|(\equiv X). \end{aligned} \tag{39}$$

The random variable $X(= X_{N,T})$ corresponding to the whole expression on the right side of the inequality in (39) is $o_p(1)$ as each term is a multiplication of $o_p(1)$ and $O(1)$ under the benchmark assumptions and the estimation procedure in Section 4.1: $\|\hat{\Sigma}_y^{-1} - \Sigma_y^{-1}\| = o_p(1)$ and $\|\hat{\Sigma}_u - \Sigma_u\| = o_p(1)$ stated in Fan et al. (2013). $\|\hat{P}_1\hat{P}_1' - P_1P_1'\| \le \|\hat{P}_1\hat{P}_1' - \tilde{P}_1\tilde{P}_1'\| + \|\tilde{P}_1\tilde{P}_1' - P_1P_1'\|$ where $\tilde{P}_1\tilde{P}_1'$ the K_1 principal subspace of $\Sigma_{y,1}$. By $\sin\theta$ theorem of Davis and Kahan (1970) $\|\hat{P}_1\hat{P}_1' - \tilde{P}_1\tilde{P}_1'\| = o_p(1)$ as $\|\hat{\Sigma}_{\chi,1} - \Sigma_{y,1}^{K_1}\| = o_p(N)$, $\lambda_{\chi,1}^{K_j} = O(N)$ and $\hat{\Sigma}_{\chi,1}$ is rank K_j. By the same theorem, $\|\tilde{P}_1\tilde{P}_1' - P_1P_1'\| = o(1)$ as $\|\Sigma_{u,1}\|$ is bounded by Assumption 2. $\|\Sigma_y^{-1}\|$ and $\|\Sigma_u\|$ are assumed to be $O(1)$ in the benchmark model, and the operator norm of a projector $\|P_1P_1'\| = 1$.
As $\Pr(X_{N,T} < \delta) \le \Pr\left(\|\hat{\mathcal{I}} - \mathcal{I}\| < \delta\right)$ for any $\delta > 0$, $\|\hat{\mathcal{I}} - \mathcal{I}\| = o_p(1)$. □

The remaining part of the proof of the main statement can proceed the same as the proof of Corollary 1 in Brownlees and Mesters (2021). First, for any $i \in \mathcal{N}$, we know that $\left|\|\hat{\mathcal{I}}_i\| - \|\mathcal{I}_i\|\right| \le \|\hat{\mathcal{I}} - \mathcal{I}\| = o_p(1)$. Second, the probability of the compliment of the event Υ is

$$\Pr(\Upsilon^c) \le N \max_{g\in\mathcal{G}, i\in\mathcal{N}^c} \max_{\ell=g,i} \Pr\left(\left|\|\hat{\mathcal{I}}_l\| - \|\mathcal{I}_l\|\right| > \delta\right),$$

where $\delta \equiv (\|\mathcal{I}_g\| - \|\mathcal{I}_i\|)/2 > 0$ for any $g \in \mathcal{G}$ and $i \in \mathcal{N}^c$ (page 8 of the Web-Appendix of Brownlees and Mesters (2021)). As $\left|\|\hat{\mathcal{I}}_i\| - \|\mathcal{I}_i\|\right| = o_p(1)$, for any $\epsilon = o(N^\gamma)$ for $\gamma < -1$,

$$\Pr\left(\left|\|\hat{\mathcal{I}}_l\| - \|\mathcal{I}_l\|\right| > \delta\right) < \epsilon$$

for large enough N. Hence $\Pr(\Upsilon^c) = o(1)$, that is, $\Pr(\Upsilon) \to 1$ as $N \to \infty$. □

B Covariance Dynamics and Factor Space Change

This section aims to provide extended comments on the benchmark model 2.1.1. We discuss how the characteristic of covariance dynamics stated in Assumption 4 is aligned with the hypothesized factor structures in both regimes stated in Assumptions 1 and 2. Especially the substantiality of the off-diagonal perturbation can be, in fact, proven, although it was simply stated as an assumption to avoid lengthy extra discussions in the main section.

Let us first recall some facts on the subspace representation to assist our discussion. As employed in Davis and Kahan (1970) as well, one of the most popular ways of identifying a linear space $\text{span}(P_j)$ is to identify it by $P_j P_j'$, the projector operator on the space $\text{span}(P_j)$ itself. In practice, it is convenient to identify $\text{span}(P_j)$ by any chosen column orthonormal basis P_j (i.e.,$P_j' P_j = I_{K_j}$) up to K_j–dimensional orthogonal transformation $\mathcal{O}$; the projector operator is invariant under any internal rotation done by $O \in \mathcal{O}$, such that $P_j O O' P_j' = P_j P_j'$ as $O'O = OO' = I_{K_j}$. P_j is called a *Stiefel* matrix and extensively studied; we refer Edelman et al. (1998) or Chikuse (2003) for a short or an extensive introduction, respectively.

For a pair of Stiefel matrices P_0 and P_1, we can decompose P_1 into the direction of the $\text{span}(P_0)$ and the $\text{span}(P_0)^\perp$, as in Section 3.2.1 of Chikuse (2003). As $K_j << N$, we state for the cases (i) $K_1 \leq K_0 < N - K_0$ and (ii) $K_0 < K_1 < N - K_0$.

Proporties 2. [Theorem 3.2.1 (i),(ii) of Chikuse (2003)]

(i) Let $K_1 \leq K_0 < N - K_0$. Then there exists Stiefel matrices $H_{K_0 \times K_1}$ and $V_{N \times K_1}$, a diagonal matrix $T_{K_1 \times K_1}$ with each diagonal element $t_h \in (0, 1)$, an orthogonal transformation $O \in \mathcal{O}(K_1)$ such that

$$P_1 = P_0 H T O' + V S O' \tag{40}$$

where $S \equiv (I - T^2)^{1/2}$ and $P_0' V = \mathbf{0}_{K_0 \times K_1}$.

(ii) Let $K_0 < K_1 < N - K_0$. Then there exists a Stiefel matrix $V_{N\times K_1}$, a diagonal matrix $T_{K_0\times K_0}$ with each diagonal element $t_h \in (0,1)$, orthogonal transformations $H \in \mathcal{O}(K_0)$ and $O \in \mathcal{O}(K_1)$ such that,

$$P_1 = P_0[H \ \mathbf{0}_{K_0\times(K_1-K_0)}]\,\mathrm{diag}\big(T, \mathbf{0}_{K_0\times(K_1-K_0)}\big)O' + VSO' \tag{41}$$

where $S \equiv \mathrm{diag}((I - T^2)^{1/2}, I_{K_1-K_0})$ and $P_0'V = \mathbf{0}_{K_0\times K_1}$. ($\mathrm{diag}(A, B)$ denotes a block diagonal matrix with matrices A and B on the diagonal.)

As discussed in Section 3.3, what matters to measure the distance of the factor spaces is the component of P_1 – up to orthogonal transformation $\mathcal{O}(K_1)$ – that is orthogonal to $\mathrm{span}(P_0)$. The expressions (40) and (41) provide enough to describe the necessary information of factor space dynamics. In other words, one can derive the expression of the factor space change invariant under the choice of basis P_0 and P_1 from (40) or (41). First, let us note that the original result Theorem 3.2.1 of Chikuse (2003) is about the decomposition of a Stiefel matrix P_1 on $\mathrm{span}(P_0)$ and $\mathrm{span}(P_0)^\perp$. The results are meant to be universal under the choice of basis P_0. For an arbitrarily chosen basis P_0, the second component in (40) or (41) corresponds to the projection of P_1 on $P_0^\perp P_0^{\perp\prime} \equiv I - P_0P_0'$, that is, $VSO' = P_0^\perp P_0^{\perp\prime} P_1 = P_0^\perp P_0^{\perp\prime} VSO'$ where S is defined respectively for case (i) and (ii). In any cases, $P_0^\perp P_0^{\perp\prime} V = V$ and the expression of V is invariant of the choice of the regime 0 basis P_0.

Besides, (40) and (41) lead universal results for the decomposition of *any* column orthonormal basis representation P_1 of $\mathrm{span}(P_1)$. If one considers a basis representation $\tilde{P}_1 = P_1\bar{O} \in \mathcal{O}(K_1)$, the decompositions will remain fundamentally the same, with $\tilde{O} \equiv O'\bar{O} \in \mathcal{O}(K_1)$ multiplied on the right end of the each terms of (40) and (41). It gives $P_0^\perp P_0^{\perp\prime} P_1 P_1' P_0^\perp P_0^{\perp\prime} = VS^2V'$ which is invariant under this internal symmetry $\mathcal{O}(K_1)$ as it is indeed supposed to be as a measure of factor space change.

Hence we can take (40) or (41) as the model of factor space dynamics for a given initial $\mathrm{span}(P_0)$. The resulting dynamics resembles a rotating position vector in Euclidean space, in a sense that there are the direction of change V and the size of the change S governing the motion from $\mathrm{span}(P_0)$ to $\mathrm{span}(P_1)$. Analogous to the motion of a rotating vector, S captures the information of the principal angles (Θ) between two subspaces; $S = \sin\Theta$, more precisely. Accordingly, T or $\mathrm{diag}\big(T, \mathbf{0}_{K_0\times(K_1-K_0)}\big)$ in (40) or (41) squares to $C \equiv \cos\Theta = (I - S^2)^{1/2}$. We refer to Davis and Kahan (1970) for an extensive discussion and interpretation.

In a matrix form, (40) or (41) can be written as follows:

$$P_1 = \begin{bmatrix} P_0 & P_0^\perp \end{bmatrix} \begin{bmatrix} \tilde{H}CO' \\ \tilde{V}SO' \end{bmatrix} \tag{42}$$

where $\tilde{V} \equiv P_0^{\perp\prime} V$, and $\tilde{H} \equiv H$ for the case (i) and $\tilde{H} \equiv [H\ \mathbf{0}]$ for the case (ii). Together with Assumptions 1 to 3 in Section 2.1, it implies that up to $o(1)$ error, the regime 1 covariance matrix will be written in terms of $[P_0\ P_0^{\perp}]$ basis such that

$$\begin{aligned}\Sigma_{y,1} &\simeq \begin{bmatrix} P_1 & P_1^{\perp} \end{bmatrix} \begin{bmatrix} \Lambda_{1,1} & \mathbf{0}_{K_1,N-K_1} \\ \mathbf{0}_{N-K_1,K_1} & \Lambda_{2,1} \end{bmatrix} \begin{bmatrix} P_1' \\ P_1^{\perp\prime} \end{bmatrix} \\ &= \begin{bmatrix} P_0 & P_0^{\perp} \end{bmatrix} \begin{bmatrix} \tilde{H}CO' & F_1 \\ \tilde{V}SO' & F_2 \end{bmatrix} \begin{bmatrix} \Lambda_{1,1} & \mathbf{0} \\ \mathbf{0}' & \Lambda_{2,1} \end{bmatrix} \begin{bmatrix} OC\tilde{H}' & OS\tilde{V}' \\ F_1' & F_2' \end{bmatrix} \begin{bmatrix} P_0' \\ P_0^{\perp\prime} \end{bmatrix}. \end{aligned} \tag{43}$$

where $P_1^{\perp} = [P_0\ P_0^{\perp}][F_1'\ F_2']'$ for some bounded operator F_1 and F_2. That is, for the perturbation Z which is assumed to exist in Assumption 4 of 2.1.1, its off-diagonal component $P_0'ZP_0^{\perp}$ is of size $O(N)$ to generate the size $O(N)$ dominating eigenvalues in regime 1 in the P_1 direction.

Properties 3. Let the benchmark Assumptions 1 to 3 hold. Assume there exists a perturbation Z such that $\Sigma_{y,1} = \Sigma_{y,0} + Z$. Then $\|P_0'ZP_0^{\perp}\|_F = O(N)$.

Proof. The upper right block of the off-diagonal perturbation with respect to the P_0 basis is $P_0'ZP_0^{\perp} = \tilde{H}CO'\Lambda_{1,1}OS\tilde{V}' + F_1\Lambda_{2,1}F_2'$ from (43). Let us denote $A \equiv \tilde{H}CO'\Lambda_{1,1}OS\tilde{V}'$ for simplicity. By Assumptions 1 to 3, $\|\Lambda_{1,1}\| = O(N)$ and $\|\Lambda_{2,1}\| = O(1)$. By Triangle inequality

$$\|A\|_F - \|F_1\Lambda_{2,1}F_2'\|_F \le \|P_0'ZP_0^{\perp}\|_F \le \|A\|_F + \|F_1\Lambda_{2,1}F_2'\|_F. \tag{44}$$

Observe that

$$\mathrm{tr}(A'A) = \mathrm{tr}\big(\tilde{V}SO'\Lambda_{1,1}OC^2O'\Lambda_{1,1}OS\tilde{V}'\big) = \mathrm{tr}\big(O'\Lambda_{1,1}OC^2O'\Lambda_{1,1}OS^2\big)$$

due to the cyclic invariance of the trace operator and the orthonormality of $\tilde{H}$ and $\tilde{V}$. It gives that

$$\min_h(\sin^2\theta_h)\mathrm{tr}\big(O'\Lambda_{1,1}OC^2O'\Lambda_{1,1}O\big) \le \mathrm{tr}(A'A) \le \max_h(\sin^2\theta_h)\mathrm{tr}\big(O'\Lambda_{1,1}OC^2O'\Lambda_{1,1}O\big),$$

which leads to

$$\min_h(\sin^2\theta_h)\min_k(\lambda_k^2)\mathrm{tr}(C^2) \le \mathrm{tr}(A'A) \le \max_h(\sin^2\theta_h)\max_k(\lambda_k^2)\mathrm{tr}(C^2),$$

where λ_k is the k–th diagonal element of $\Lambda_{1,1}$. Under the assumed factor structure of regime 1, $\min_k(\lambda_k^2)$ and $\max_k(\lambda_k^2)$ are $O(N^2)$. By Properties 2, $\min_h(\sin^2\theta_h) > 0$ and $\mathrm{tr}(C^2) > 0$. Hence $\|A\|_F = O(N)$ and so is $\|P_0'ZP_0^{\perp}\|_F$ as in (44).

□

C A Network-based Interpretation of Latent Factor Models

Let us consider a system of N individual series $\mathbf{y}_t = [y_{1t}, \ldots, y_{Nt}]'$. During a time window $\mathtt{I}_0$, the cross-sectional items are interconnected by a constant relationship Ω and experience minor idiosyncratic fluctuations u_{it}. The interconnections can arise due to mutual investments (including buyer-seller relationships) or borrower-lender relationships or implying an indirect manifestation of holding similar investment portfolios. Assume, for simplicity, that the interconnected performances are balanced with one common source of exposure, r. It can be a final good demand or a common return from a safe investment. That is, for $t \in \mathtt{I}_0$,

$$y_{it} - u_{it} = r_t + \sum_j \Omega_{ii'}(y_{i't} - u_{i't}), \quad \text{or equivalently,}$$

$$\mathbf{y}_t = (I_N - \Omega)^{-1}\mathbf{1}r_t + \mathbf{u}_t = \mathbf{b}r_t + \mathbf{u}_t. \tag{6}$$

Note that, in this example of a single common exposure,

$$\mathbf{b} \equiv (I_N - \Omega)^{-1}\mathbf{1},$$

which equals the Bonacich centrality of the cross-sectional items in the constant network Ω. When the common source of exposure and the interconnected structure Ω are not observable, one can describe (6) by a one-dimensional latent factor model,

$$\mathbf{y}_t = \tilde{B}f_t + \mathbf{u}_t$$

where the factor loading $\tilde{B}$ amounts to the centrality vector $\mathbf{b}$, up to unknown scalings. The idiosyncratic errors $\{\mathbf{u}_{it}\}$ can capture any individual unit-specific disturbances. For example, for a panel of firms, such disturbances can be caused by a sudden reputation or leadership change in a single or group of companies, which can be seen as a change in the value of organizational capital. One can think of the Enron scandal during the dot-com bubble in 2000 and the ownership change of Twitter(X) in 2022, all able to cause fluctuations in sales or stock returns of certain units. Besides, as a given system of N cross-section units rarely includes all relevant economic agents in relation, any disruption of a relationship of i to an entity outside of the system in consideration will be captured as an idiosyncratic error.

For the granular units, idiosyncratic disturbances can trigger a viable adjustment of the internal relationships represented by Ω. For example, a bank or a firm can perceive idiosyncratic volatilities of their own (or around) as a subjective risk factor of mutual

investment. If they make an assessment that the expected disturbances are above a certain level, they can try to adjust their investment portfolio to absorb or mitigate the potential risk.[19] As granular units adjust relationships around, Ω is altered, and naturally, all the coefficients of the centrality vector $\mathbf{b}$ change, not trivially, such as a mere change of the scaling. It will be perceived as a change of the one-dimensional factor space to another, say $\mathcal{P}_1$. The one-dimensional factor model based on (6) has just provided insight into an observable characteristic of the granular units while staying agnostic without specifying the exact mechanism for how the idiosyncratic disturbances can bridge in the factor space adjustment.

The next regime centrality, say $\mathbf{b}_1$, or its counterpart $\tilde{B}_1$ or $\mathcal{P}_1$ under unobservability, does not necessarily have a direct functional dependence on the idiosyncratic second moments that may trigger the adjustment. The actual adjustment of linkages, hence the coefficients of $\mathbf{b}_1$ or $\mathcal{P}_1$ can depend on parameters indicating the capability of the adjustment – such as market or bargaining power, or information superiority of some units, or system-wide asymmetry of those – rather than the idiosyncratic second moments indicating the demand of an adjustment.

In the most simplified example below, where we assume the common exposure variance is a large constant compared to hypothetically homogeneous idiosyncratic variances, the suggested influence measure detects an individual i to have a system-wide importance if it adjusts its centrality the most.

Example 1. Let $\mathbf{y}_t = \mathbf{b}r_t + \mathbf{u}_t$, where $\text{cov}(\mathbf{u}_t) = I_N$ during $\mathtt{I}_0$. Assume that $\text{var}(r_t) = \sigma_r^2 \gg 1$ is constant regardless of the regime. It gives $\Sigma_{\mathbf{y}} = \sigma_r^2\mathbf{b}\mathbf{b}' + I$ and $\Sigma_{\mathbf{y}}^{-1} = I_N - \sigma^2\mathbf{b}\mathbf{b}'/(1+\sigma_r^2\mathbf{b}'\mathbf{b})$. Then the i–th column norm $\mathcal{I}_i = \left\|\Sigma_{\mathbf{y}}^{-1}\mathbf{b}_1\mathbf{b}_1{}'\Sigma_{\mathbf{y}}^{-1}\boldsymbol{\sigma}_u^i\right\|$ is the largest if

$$\left[b_{i,1} - \frac{\sigma_r^2\mathbf{b}_1{}'\mathbf{b}}{1+\sigma_r^2\mathbf{b}'\mathbf{b}}b_i\right]^2$$

is the largest. As $\mathbf{b}_1{}'\mathbf{b}$ is a scalar common to all i, it implies that the one that changes its centrality the most is the systemic individual. It aligns with our view that a centrality change in any direction is a manifestation of network structure change, which is a result of strategic decisions. In some sense, an adjustment could indicate one's relative vulnerability. However, in any case, it will be better considered as a potential risk component

[19] In a financial network, it could be assumed to keep the leverage level the same as the perceived value at risk. e.g., Mazzarisi, Lillo, and Marmi (2019).

of a given system.[20]

Now, let us consider general cases with multiple (K) sources of common exposure:

$$y_{it} - u_{it} = \sum_k \alpha_{ik} r_{k,t} + \sum_j \Omega_{ij}(y_{jt} - u_{jt}), \quad \text{or,}$$

$$\mathbf{y}_t = (I_N - \Omega)^{-1} A \mathbf{r}_t + \mathbf{u}_t = \left[(I_N - \Omega)^{-1}\boldsymbol{\alpha}^1 | \cdots | (I_N - \Omega)^{-1}\boldsymbol{\alpha}^K\right]\mathbf{r}_t + \mathbf{u}_t = B\mathbf{r}_t + \mathbf{u}_t, \tag{45}$$

where a nonnegative matrix of marginal benefits $A_{NK} = [\alpha_{ik}]$, whose $k-$th column is $\boldsymbol{\alpha}^k$. As Ω,A and $\mathbf{r}_t$ are latent, and the $\{r_k\}$ are strong, it will be described by the $K-$dimensional factor model $\mathbf{y}_t = P\mathbf{f}_t + \mathbf{u}_t$. Each column of B consists of a weighted Bonacich centrality $\mathbf{b}^k \equiv (I_N - \Omega)^{-1}\boldsymbol{\alpha}^k$ (Ballester et al. (2006)). It can be seen as an equilibrium action of exposure to r_k of a simple game (Ballester et al. (2006), Galeotti et al. (2020))

$$\max U_i^k(b_{ik}) = \max\left[b_{ik}\alpha_{ik} - (1/2)b_{ik}^2 + b_{ik}\sum_j \Omega_{ij} b_{jk}\right] \quad \text{for all } k$$

where the payoff from action is correlated to the others' action through Ω, and marginal benefits are given as α_{ik}.

For the point on our criteria of the number of granular units, if one tries to adjust their action, it will affect all others' equilibrium action as for each r_k, the actions depend on others' action. Hence, we take the number of common sources whose equilibrium is adjusted as a conservative measure of the number of systemic individuals. Note that the true number of the common source can be larger than the number of latent factors or the dimension of the factor space, as only a subset of $\{r_k\}$ gives strong enough signals. If there is a significant adjustment in the equilibrium for a week $\{r_k\}$ can be seen as an advert of a new factor.

In the following simplified example, the influence measure gives individuals with the largest changes in action as the granular units, with an additional consideration of how the exposures for different sources are overall correlated.

[20]The exact extension of this interpretation can be made only in restrictive scenarios in general cases with multiple sources of exposures – we will discuss soon; for example, where the N agents are partitioned into K different groups $\{G_k\}$ by different common exposures, ($\alpha_{ik} = \mathbf{1}_{i\epsilon G_k}$) and the group does not change across regimes. In this particular case, the systemic individuals are the ones with the largest centrality change in each group. In general cases, we will have an interpretation in terms of weighted centrality or equilibrium actions of a game of exposures. We will soon discuss this.

Example 2. Let $\mathbf{y}_t = B\mathbf{r}_t + \mathbf{u}_t$, where $\text{cov}(\mathbf{u}_t) = I_N$ during $\mathtt{I}_0$. Let $\text{cov}(\mathbf{r}_t) = \sigma_r^2 I_K$ overall time, for $\sigma_r^2 \gg 1$. Then $\Sigma_{\mathbf{y}} = \sigma_r^2 BB' + I_N$ and $\Sigma_{\mathbf{y}}^{-1} = I_N - \sigma_r^2 B(I_K + \sigma_r^2 B'B)^{-1}B'$. The $i-$th column norm $\mathcal{I}_i = \left\|\Sigma_{\mathbf{y}}^{-1} B_1 B_1{}' \Sigma_{\mathbf{y}}^{-1} \boldsymbol{\sigma}_u^i\right\|$ is the largest if

$$\sum_k \left[b_{i,1}^k - \sigma_r^2 \mathbf{b}_1^{k\prime} B(I_K + \sigma_r^2 B'B)^{-1}\mathbf{b}_i\right]^2$$

is the largest. Further, let $B'B = I_K$ to simplify interpretation. The measure of the change of individual's action for $k-$th source of exposure has an extra consideration on how regime1 action of all $\mathbf{b}_1^k$ is correlated to regime 0 actions $\mathbf{b}_0^\kappa$ for all κ, captured by $\mathbf{b}_1^{k\prime} B$. That us, a player i's regime 1 action for each $k-$th exposure $b_{i,1}^k$ is compared to its own action for all κ in the regime 0 ($\mathbf{b}_i$) weighted by the overall similarity of actions across regimes. The change in one's action will be depreciated if actions across regimes overall correlate in the same direction as the individual change. If the chosen action of i is co-moving with most of all others, the resulting magnitude of change will get a penalty.

In general cases, the measure and interpretation of individuals' importance are based on their actions. It is the combination of an underlying network and marginal benefits on direct exposures to $\{r_k\}$. Those factors are jointly determining the correlation structure among cross-sectional items. Our criterion of detection parallels to identify individuals changing the most of their actions, net of the overall comovement of actions.
We close this discussion by presenting the following example, where the change of actions can be visualized as a change in the underlying network.

Example 2.a Let $N = 100$ and $K = 3$. Assume $\mathbf{u}_t \sim \mathcal{N}(\mathbf{0}, 2I_N)$, and $\mathbf{f}_t \sim \mathcal{N}(\mathbf{0}, 25I_K)$ for all t. We consider, for simplicity, a case where N agents can be partitioned into K groups regarding the direct exposure to different source r^k. For instance, let the N by K matrix A of the direct exposure coefficients be given as [21]

$$A = \begin{bmatrix} \mathbf{0} & \mathbf{0} & \mathbf{1}_{20} \\ \mathbf{1}_{30} & \mathbf{0} & \mathbf{0} \\ \mathbf{0} & \mathbf{1}_{50} & \mathbf{0} \end{bmatrix}, \tag{46}$$

where $\mathbf{1}_m$ denotes a length m column vector of ones. It is additionally assumed to be fixed across regimes. Then the units of individuals (nodes) $3, 22$, and 55 are the most important in the following change of underlying network structure, from left to right of Figure 11:

[21] Or it can be $A\mathcal{O}_K$ for any orthogonal transformation $\mathcal{O}_K$

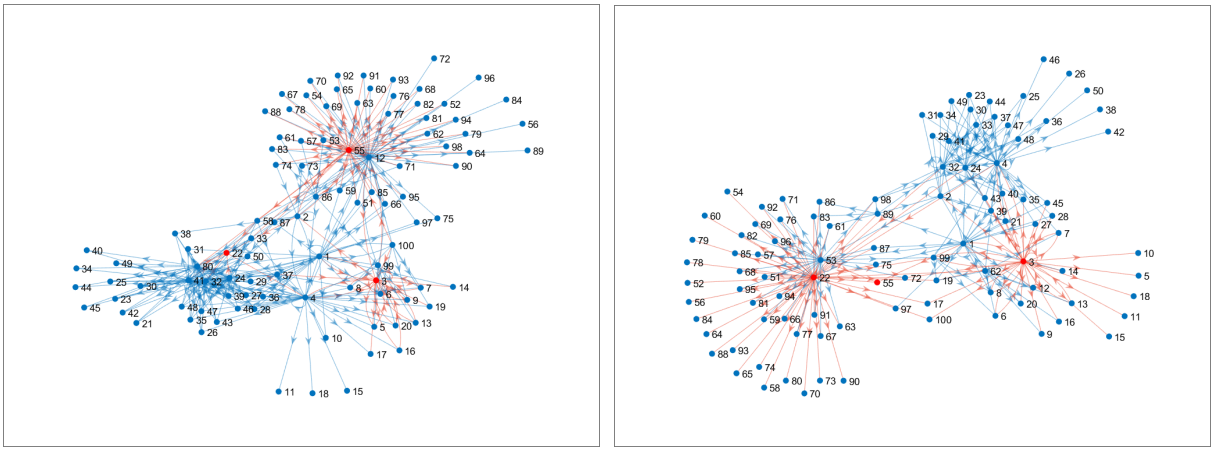

(a) Ω (b) Ω_1

Figure 11

In this example, by fixing A in the form (46), the change in action $\mathbf{b}_i$ coincides with changes of importance in propagating the effect of its direct exposure(to some r^k) to all. The graphical description of degree centrality can broadly capture the latter due to the setup of A. The importance of node 22 is revealed by substantially gaining centrality. That of node 55 is the opposite, by substantially losing centrality. Node 3 is counted as important as its centrality spreads to a collection of nodes that were not connected previously.

D A Note on the First Order Effect

It was the partial derivative of the expression

$$d\big(\text{span}(P_0), \text{span}(P_1)\big) \simeq \text{tr}\Big[\Sigma_u \Sigma_y^{-1} \mathcal{P}_1 \Sigma_y^{-1} \Sigma_u\Big] \tag{11'}$$

that enabled the measure (13) in Section 3.2. Mechanically, what we analyze is the first-order effect on the distance, which depends both on the initial state $\mathcal{P}_0$ and the new state $\mathcal{P}_1$. When we considered the first-order effect of Σ_u on this expression, $\mathcal{P}_1$ was fixed as given as it does not have a direct effect (the first order effect) from a perturbation of Σ_u. A perturbation of Σ_u effectively implies a perturbation on the initial state of the system, $\mathcal{P}_0$. It is a hypothetical perturbation on the decomposition structure of the regime-0 system covariance into the common and idiosyncratic covariance, fixing the summation. The granular units have the largest contributions through the state perturbation.

In general cases, the analysis based on the partial effect (12) can still provide a measure of systemic influence by assuming the direction (sign) of the potential direct effect on

the regime-1 factor space is the same as that of the initial state perturbation due to the perturbation on the granular units. Let us discuss this in detail for the cases where $\mathcal{P}_1$ has a direct dependence on Σ_u. Due to the cyclic invariance of the trace operator, the partial derivative gives the first-order effect of $\boldsymbol{\sigma}_u^i$ as

$$\mathring{\mathcal{I}}_i \equiv \left\| \frac{1}{2}\left[\partial_{\Sigma_u} d\big(\text{span}(P_0), \text{span}(P_1)\big)\right]^i \right\| = \left\| \Sigma_y^{-1}\mathcal{P}_1\Sigma_y^{-1}\boldsymbol{\sigma}_u^i + \Delta^i \right\|, \tag{47}$$

where

$$\Delta^i \equiv \sum_{\ell,m}^{N} \begin{bmatrix} \frac{\partial[\mathcal{P}_1]_{\ell m}}{\partial \sigma_u^{i1}} \\ \vdots \\ \frac{\partial[\mathcal{P}_1]_{\ell m}}{\partial \sigma_u^{iN}} \end{bmatrix} \left[\Sigma_y^{-1}\Sigma_u^2\Sigma_y^{-1}\right]_{m\ell}. \tag{48}$$

The Δ in (47) is infeasible to identify without a specific model of $\mathcal{P}_1$ with respect to Σ_u. We assume that the second term Δ is aligned with the first term in (47) for the granular units and misaligned for the others. That is, the direction of the potential direct effect on the regime-1 factor space is the same as that of the initial state perturbation due to $\boldsymbol{\sigma}_u^g$.

Assumption D. Denote $\mathcal{I}_i \equiv \left\| \Sigma_y^{-1}\mathcal{P}_1\Sigma_y^{-1}\boldsymbol{\sigma}_u^i \right\|$ for any $i \in \mathcal{N}$. Let us assume the following:

a) $sgn\left[\Sigma_y^{-1}\mathcal{P}_1\Sigma_y^{-1}\boldsymbol{\sigma}_u^g\right]_m = sgn(\Delta_m^g)$ for all $m \in \mathcal{N}$ for $g \in \mathcal{G}$.

b) $sgn\left[\Sigma_y^{-1}\mathcal{P}_1\Sigma_y^{-1}\boldsymbol{\sigma}_u^i\right]_m = -sgn(\Delta_m^i)$ for all $m \in \mathcal{N}$ for $i \notin \mathcal{G}$.

c) $\mathcal{I}_g > \mathcal{I}_m$ for all $g \in \mathcal{G}$ and $m \notin \mathcal{G}$.

Then $\mathring{\mathcal{I}}_g \geq \mathcal{I}_g > \mathcal{I}_i \geq \mathring{\mathcal{I}}_i$ for any $g \in \mathcal{G}$ and $i \notin \mathcal{G}$, and we detect the granular units by ranking $\{\mathcal{I}_i\}_{i\in\mathcal{N}}$ instead of $\{\mathring{\mathcal{I}}_i\}_{i\in\mathcal{N}}$.

E A Geometrical Interpretation on the Detection Criteria

The proposed scheme of detection based on the partial effect of $\boldsymbol{\sigma}_u^i$ in (13) can be explained from a more geometrical point of view aligned with the discussion in Section 3.3 and Appendix B. One can be interested in possible geometrical modeling supporting the detection scheme, in addition to the interpretations already presented in Section 2.2, Section 3, and Appendix C.

Let us start by reviewing the geometrical features of the factor space change and the benchmark criteria 3.3.1. As discussed mainly in 3.3 and Appendix B, the factor space dynamics can be seen as a rotation in $N-$dimensional space, which is determined by

two types of information: directions of change of the basis vectors $V_{N\times H}$, and angles $\Theta = \mathrm{diag}(\theta_1, \ldots, \theta_H)$ capturing how far the basis vectors rotate to the chosen directions. For any $h = 1, \ldots, H$, $\theta_h \in [0, \pi/2]$ to describe identifiable rotations.

As the factor space is a multi-dimensional object, its change is also multi-dimensional by nature, which requires several different types of information to represent it: the shape (which can be captured by directional information V), the dimension (H), and the magnitude (Θ). The distance measure itself (10) gives a gross aggregation *after* taking the trace. It captures only one type of information about the change – the overall magnitude – erasing any directional and dimensional information. We can see this point with the help of the discussion in Appendix B as

$$d\big(\mathrm{span}(P_0), \mathrm{span}(P_1)\big) \equiv \mathrm{tr}\big[P_0^{\perp} P_0^{\perp\prime} P_1 P_1{}' P_0^{\perp} P_0^{\perp\prime}\big] = \mathrm{tr}(V \sin^2\Theta V') = \sum_{h=1}^{H} \sin^2\theta_h \qquad (10')$$

where $\sin\Theta = \mathrm{diag}(\sin\theta_1, \cdots, \sin\theta_H)$ is the realized principal angles θ_h between two subspaces represented by $P_0 P_0{}'$ and $P_1 P_1{}'$.

This is one of the reasons why we propose a detection scheme by modeling the argument *inside* the trace operator defining the distance measure (10). By doing so, our detection criteria 3.3.1 utilize all three types of information representing the change of the factor space. It is important to capture the full characteristics of the factor space change in our proceedings. Especially, the directional information can provide a valuable factor to explain individual shares in the magnitude of the factor space change.

To have a closer look at this point, first recall the discussion on the directional information of the factor space change in Section 3.3. As in the paragraph above Assumption 5, what matters to capture the change of the factor space is the component of $P_1 P_1{}'$ perpendicular to $P_0 P_0{}'$, whose directional information amounts to V. The V is, approximately in large N, a choice of a size H subcollection of the eigenvectors of Σ_y^{-1} corresponding to $N - K$ largest eigenvalues – in other words, the smallest $N - K$ eigenvalues of Σ_y.[22]

Let $V = \tilde{P}_{N\times H}$ by column-augmenting a chosen set of eigenvectors $\{\tilde{\mathbf{p}}_h\}_{h=1,\ldots,H}$ of Σ_y^{-1}, and denote $\tilde{\Lambda}_y^{-1}$ the diagonal matrix of the eigenvalues of Σ_y^{-1} corresponding to the chosen eigenvectors. Combined with the discussion in Appendix B, the proposed influence measure (13) can be written as

$$\mathcal{I}_i = \left\|\Sigma_y^{-1} P_1 P_1{}' \Sigma_y^{-1} \boldsymbol{\sigma}_u^i\right\| = \left\|\Sigma_y^{-1} V D V' \Sigma_y^{-1} V' \boldsymbol{\sigma}_u^i\right\| = \left\|V \tilde{\Lambda}_y^{-1} D \tilde{\Lambda}_y^{-1} V' \boldsymbol{\sigma}_u^i\right\| \Big(= \left\|V \tilde{D} V' \boldsymbol{\sigma}_u^i\right\| \Big) \quad (13')$$

where $D \equiv \sin^2\tilde{\Theta}$, for $\tilde{\Theta}$ denoting the distance perturbed due to the first-order effect of Σ_u. That is, the directional information plays a crucial role in explaining how the magnitude

[22] More precisely, the chosen VV' is a subspace of the $N - K$ principal subspace of Σ_y^{-1}.

of the factor space change $\sin^2\tilde{\Theta}$ is decomposed into the individual shares; $\mathcal{I}_i$ measures the length of a weighted (by $\tilde{D} \equiv \tilde{\Lambda}_y^{-1} D \tilde{\Lambda}_y^{-1}$) projection of $\boldsymbol{\sigma}_u^i$ on the directions V represents. We can clearly see that the membership detection employs two types of information: the directional and the magnitude, based on the measure $\{\mathcal{I}_i\}$. The dimensional information determines the number of granular units. Hence, all three types of information are utilized for the granular unit detection in 3.3.1.